The result of the MEG experiment with the full dataset
(+ MEG II status)

Daisuke Kaneko, on behalf of

the MEG collaboration

ICEPP
The University of Tokyo

Contents

1. $\mu \rightarrow e\gamma$ Decay

2. MEG Instruments

3. Analysis and Result

4. MEG II experiment

1. $\mu \rightarrow e\gamma$ Decay

Flavor of Particles

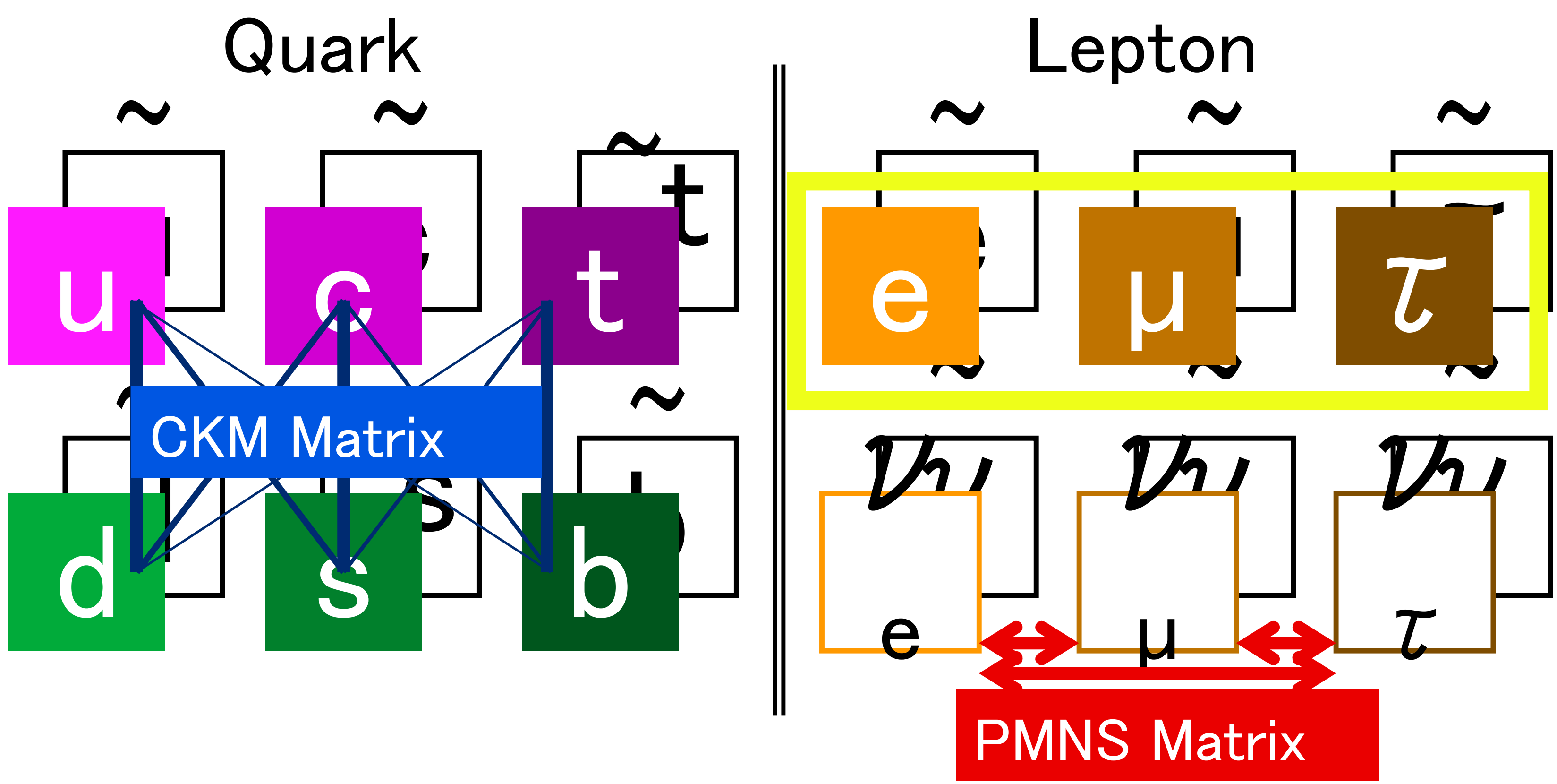

$\mu^+ \to e^+ \gamma$: undiscovered decay

- Forbidden in Standard Model (Lepton flavor conservation law)

- It is possible, with neutrino oscillation, probability is < 10^{-50} no exist practically

- Promising theories beyond SM predict accessible probability
  - see-saw mechanism
  - SUSY-GUT
  - etc.

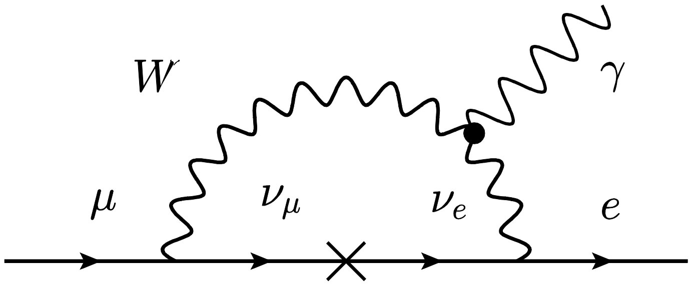

$\mu \to e \gamma$ via ν-oscillation

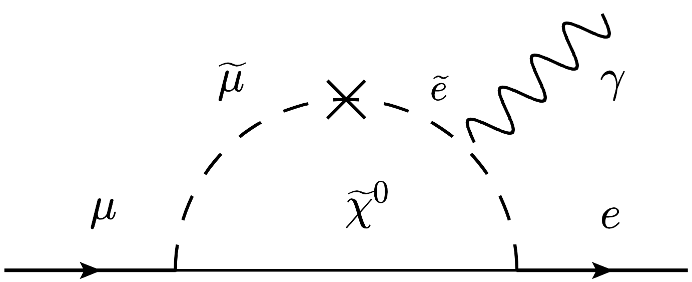

$\mu \to e \gamma$ via SUSY particle

$10^{-12} \sim 10^{-14}$ is predicted

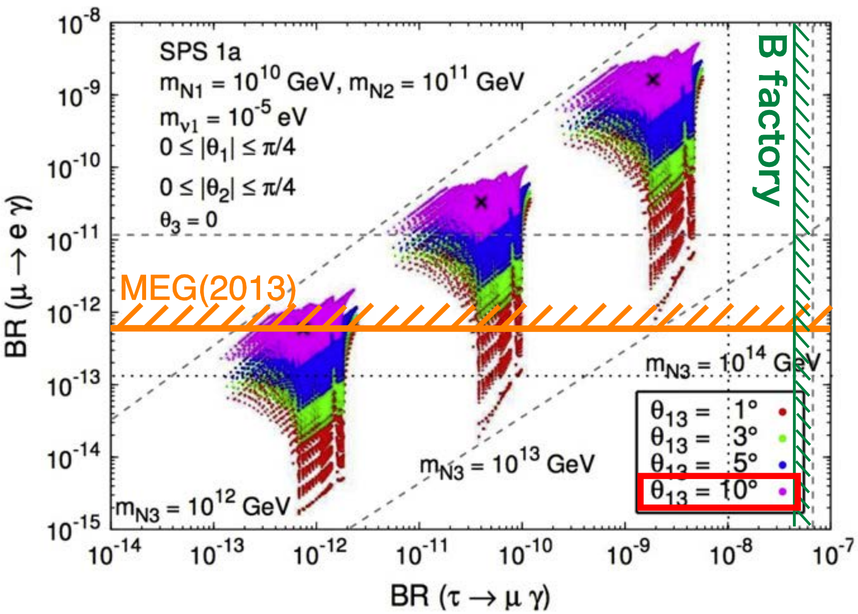

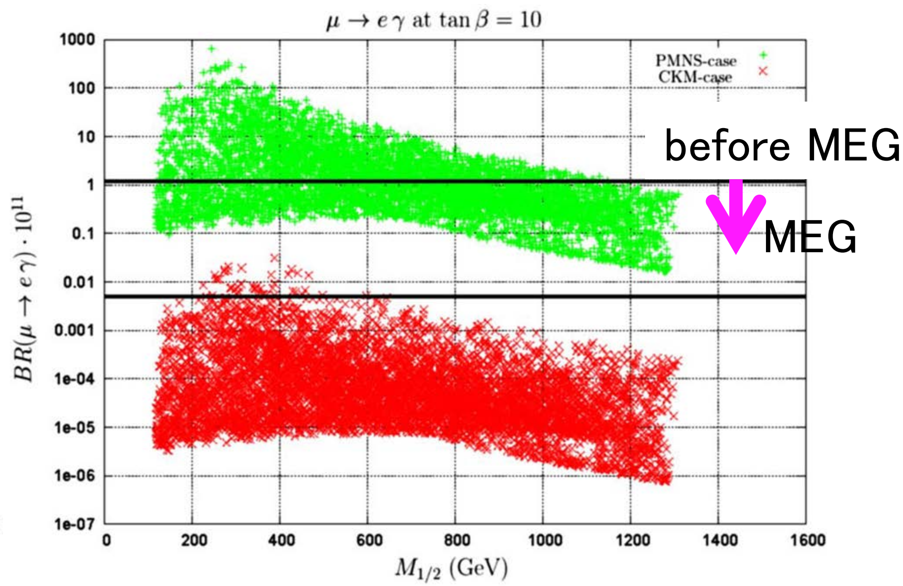

Antusch et al.,
J. HEP **2006**(11), 090 (2006)

SU(5) + seesaw
different colors correspond different θ_{13} value
(already discovered to be ~9°)

L. Calibbi et al.
Phys. Rev. D **74,** 116002 (2006)

SO(10) + seesaw
green : PMNS case, red : CKM case
$\tan\beta$ = 10, as function of $M_{1/2}$

History of $\mu \rightarrow e \gamma$ search

1936

Discovery of μ

1947

First search with cosmic-ray

○ μ is not an excited state of e

1950s

$\mu \rightarrow e \gamma$ search with accelerator

1970s

search with meson factories

○ Concept of lepton flavor

× Rumor of discovery, but not true

Crystal Box 1.7×10^{-10} 1984 @LAMPF

MEGA 1.2×10^{-11} 1999 @ LAMPF

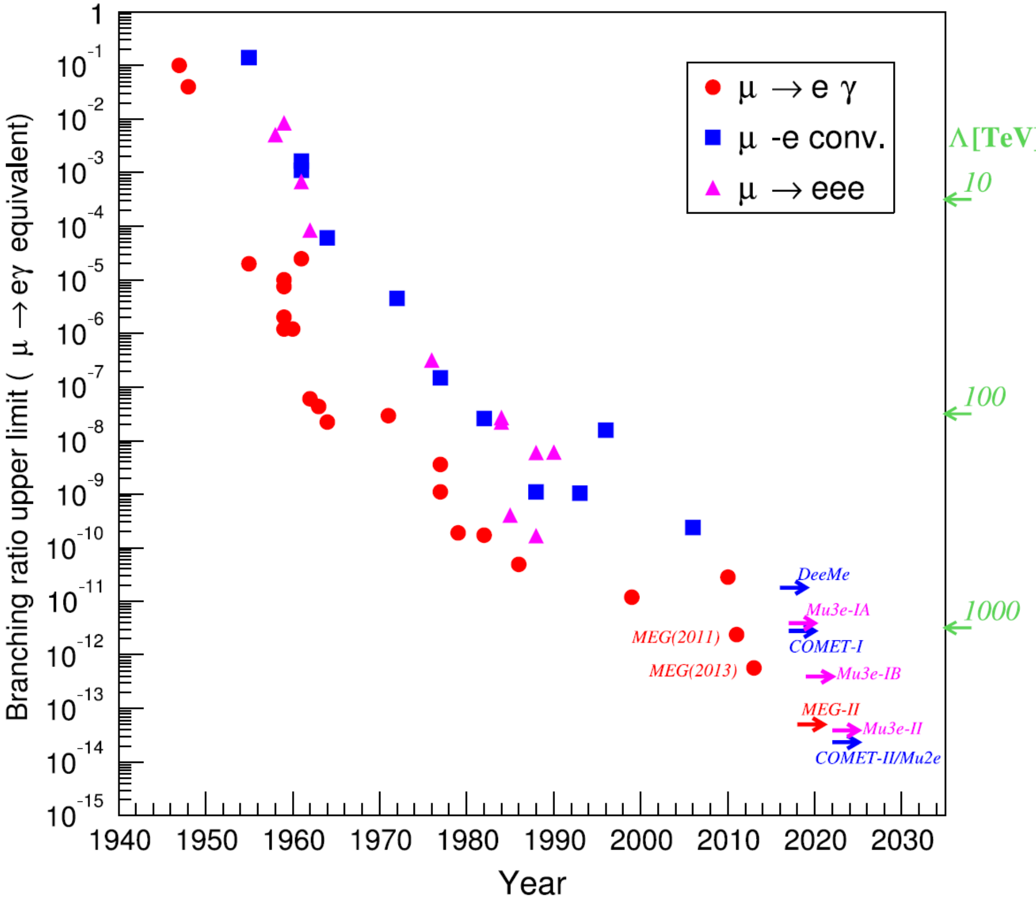

Signal & BackGround

○ Signal

52.8 MeV = m_μ /2, back–to–back, at the same time.

● BackGrounds

○ Raditive Muon Decay (RMD) $\mu^+ \rightarrow e^+ \overline{\nu_\mu} \nu_e \gamma$

○ ACCidental BG (ACC) $R_{BG} \propto R_\mu{}^2 \cdot \delta E_e \cdot (\delta E_\gamma)^2 \cdot \delta \omega / 4\pi \cdot \delta t$

– e^+ from normal μ+ decay

– γ from RMD or annihilation of e^+

Type	Eγ	Ee+	Time	Angle
Signal	52.8 MeV	52.8 MeV	Te = Tγ	180°
RMD	<52.8 MeV	<52.8 MeV	Te = Tγ	≦180°
ACC	<52.8 MeV	≦52.8 MeV	uniform	no correlate

2. MEG Instruments

Location of experiment

PSI experimental hall

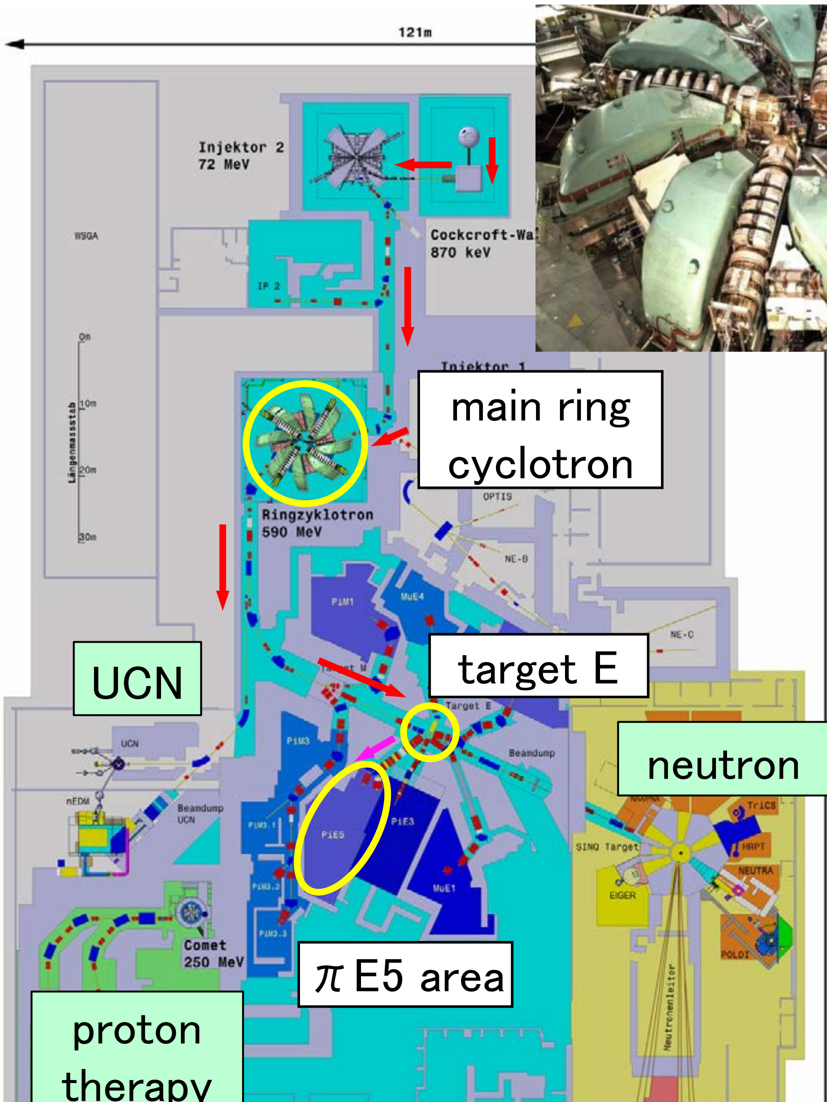

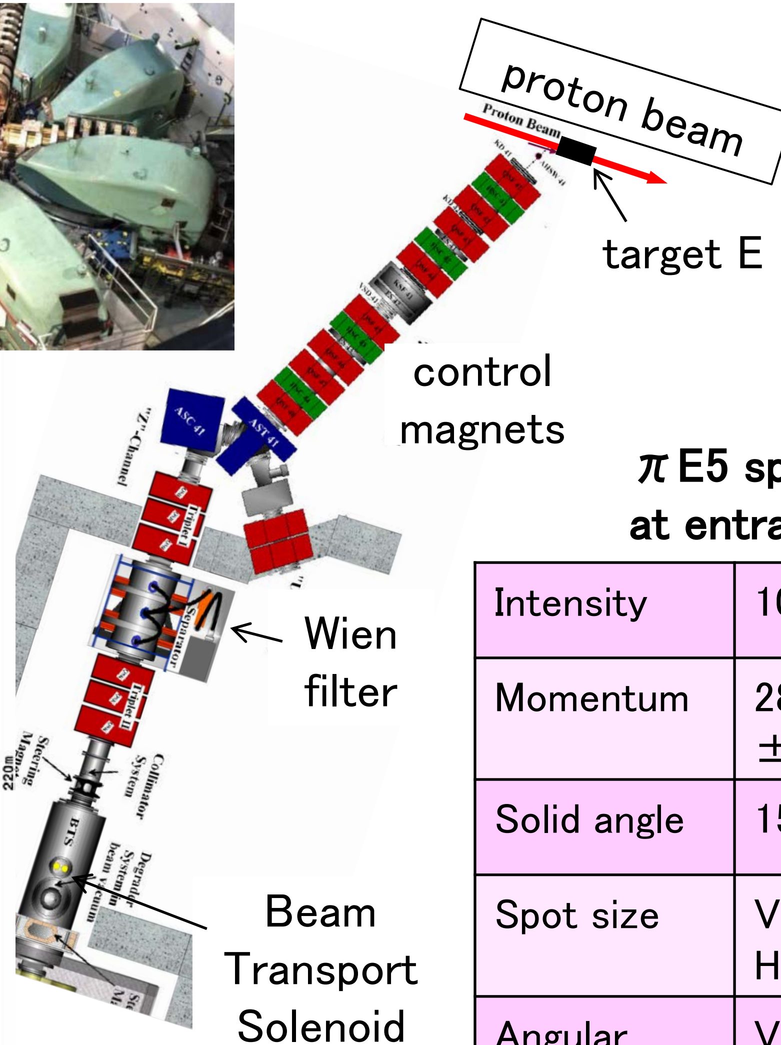

π E5 spec. at entrance

Intensity	10^8 /s
Momentum	28 MeV/c ± 5–7%
Solid angle	150 mstr
Spot size	V: 15mm H: 20mm
Angular divergence	V: 450 mrad H: 120 mrad

BTS & Target

Beam
Transport
Solenoid

He-cooled Superconducting magnet to conduct μ beam on target

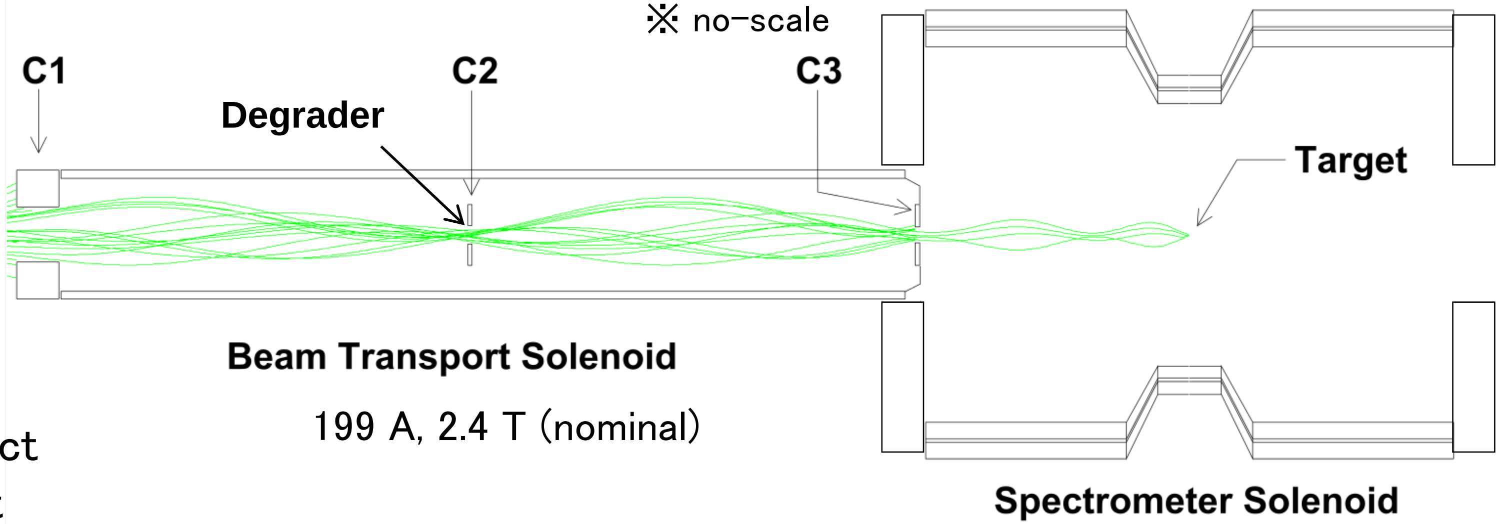

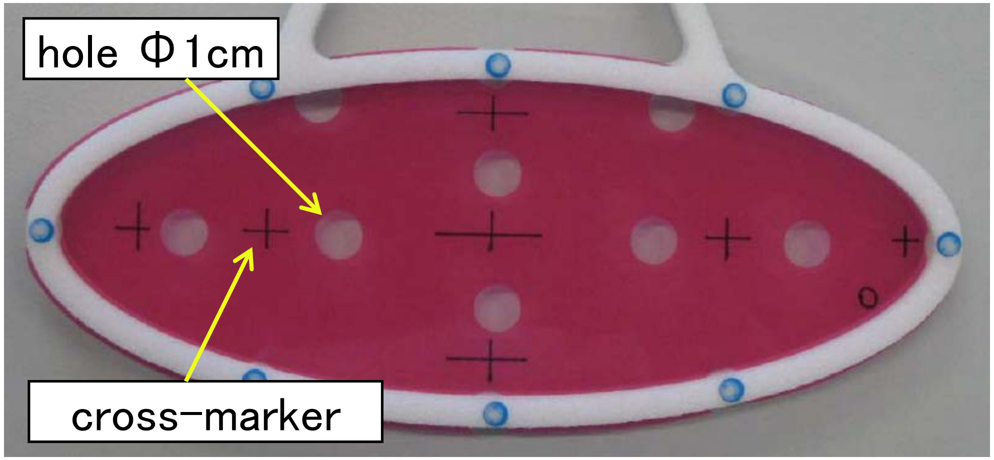

μ^+ stopping target

Requirement

Must stop μ^+, but
must not interrupt e^+
→ Put thin film with angle

Design

8 cm × 20 cm ellipse
20.5° slant angle
Stacked PE & PS, 205 μm

MEG detector

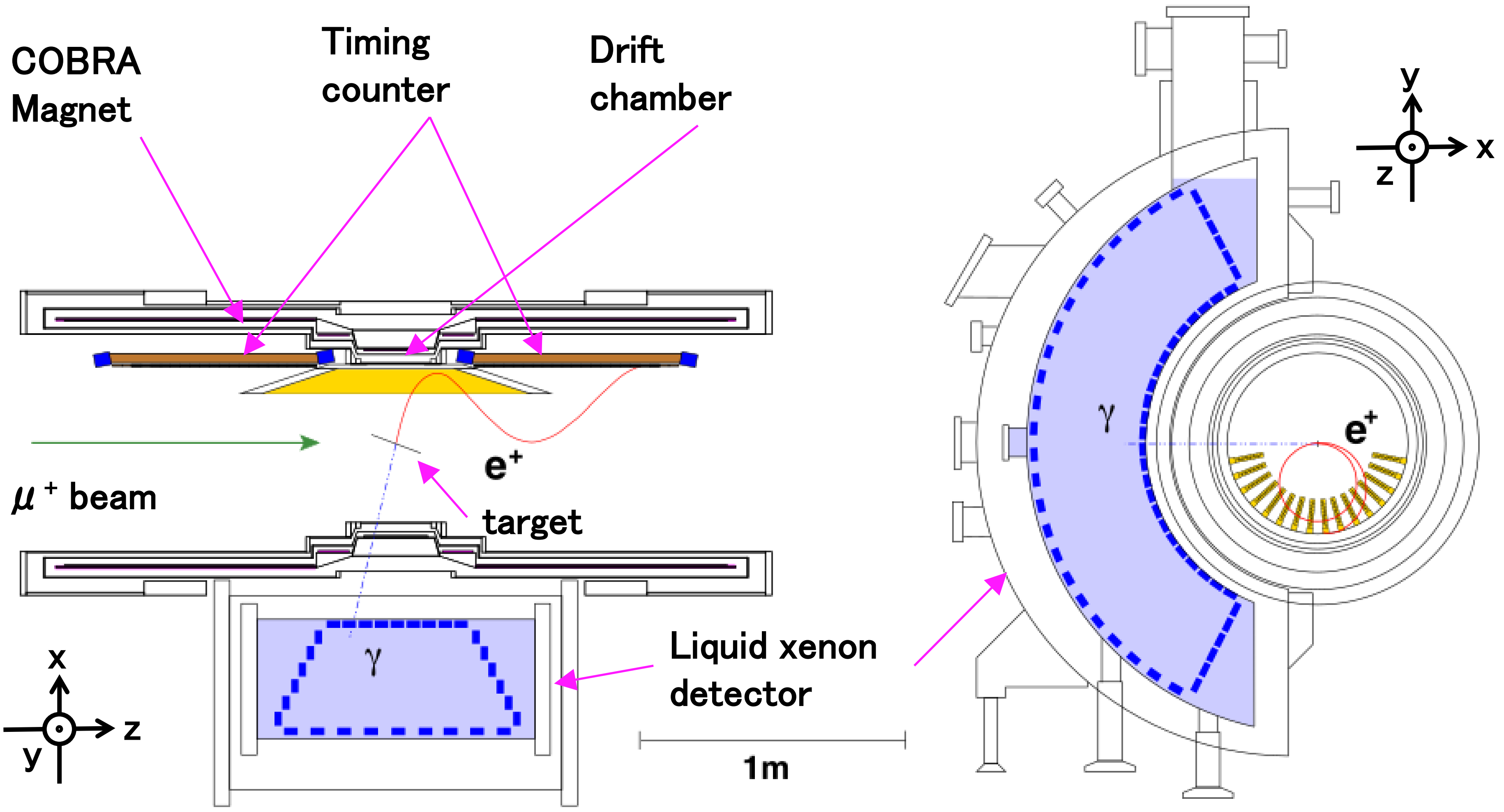

Liquid Xe γ-ray detector

Liquid Xenon ?

- Rare-gas scintillator
- Fast, Many photon
- Heavy as a liquid
- Homogeneity
- No self-absorption

→ Many applications in high-energy experiments

Difficulty in application

Handle low-temp liquid (T~165 K)

Control pressure ($\Delta P < 0.01$ atm)

Detect Ultra-violet light ($\lambda \sim 175$ nm)

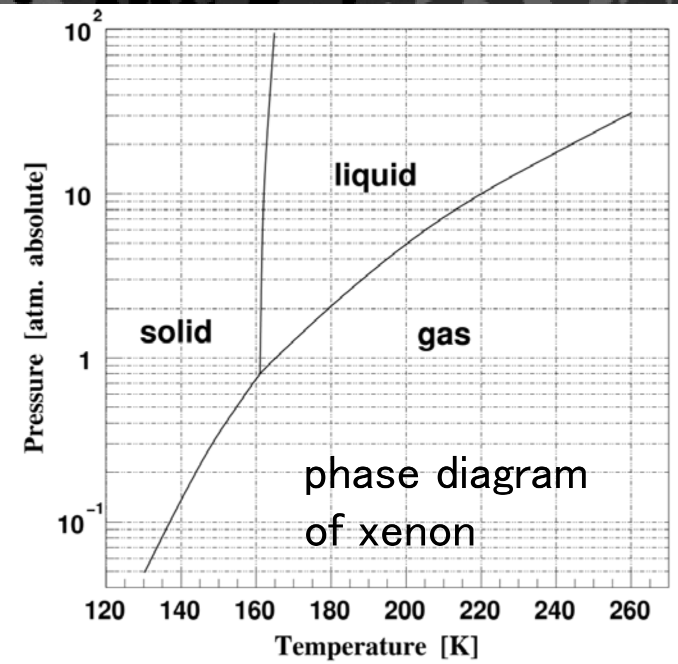

phase diagram of xenon


Hamamatsu R9869 Photo-multiplier

LXe detector design

Characteristics

・Total 900 l LXe

・C-shaped cryostat

・846 PMTs on 6 face

・Honey-comb window at γ-ray entrance face

・Cooled with pulse tube refrigerator

・2 kinds of purification systems equipped

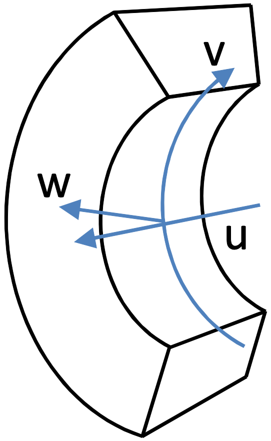

200 W pulse tube refrigerator

LXe detector γ-ray calibration

Main γ calibrations

A. Cockcroft-Walton (CW) accrlerator
   target of $Li_2B_4O_7$
   14.8, 17.6 MeV

B. Neutron generator
   Ni(n, γ)Ni reaction
   9.0 MeV

C. Charge exchange
   $\pi^- + p \rightarrow \pi^0 + n$
   $\pi^0 \rightarrow \gamma + \gamma$

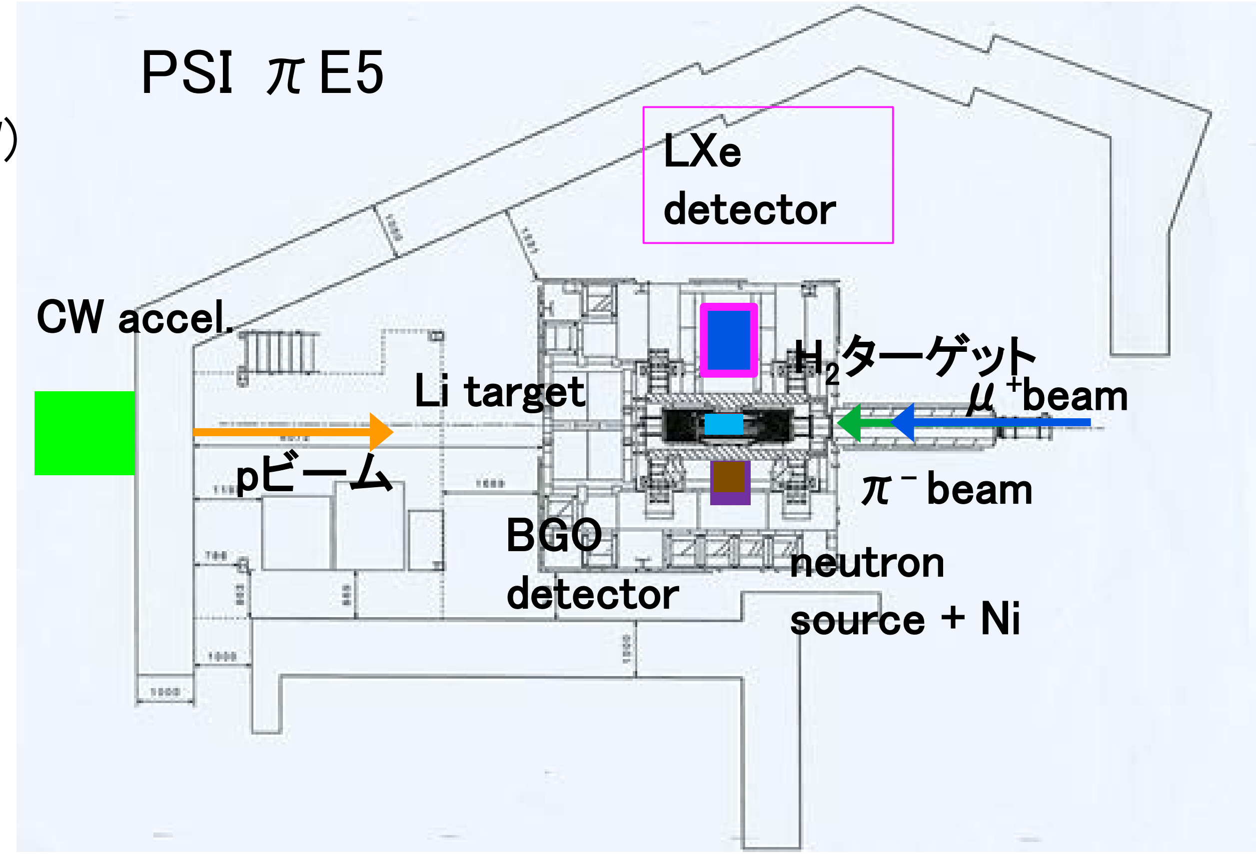

π^0 calibration

2γ from the reaction $\pi^0 \rightarrow \gamma + \gamma$

By selecting back-to-back γ pair, concentrated energy γ can be selected.

Most important calibration, since 55 MeV is near signal.

BGO detector is small and movable, to scan all acceptance of LXe.

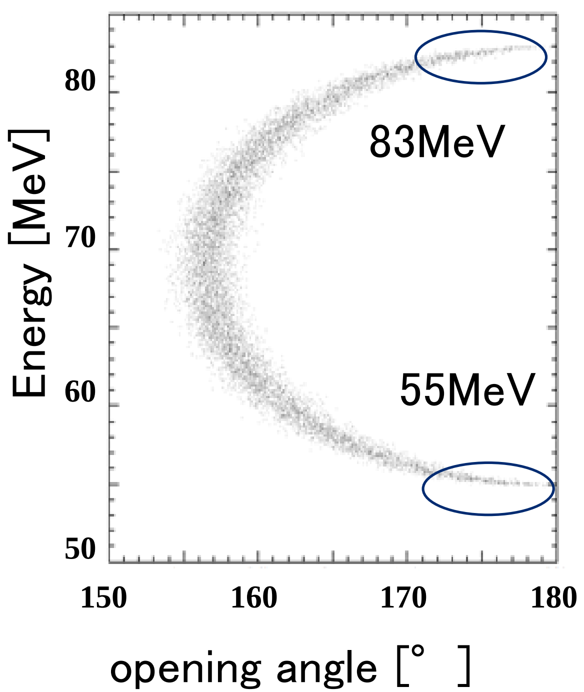

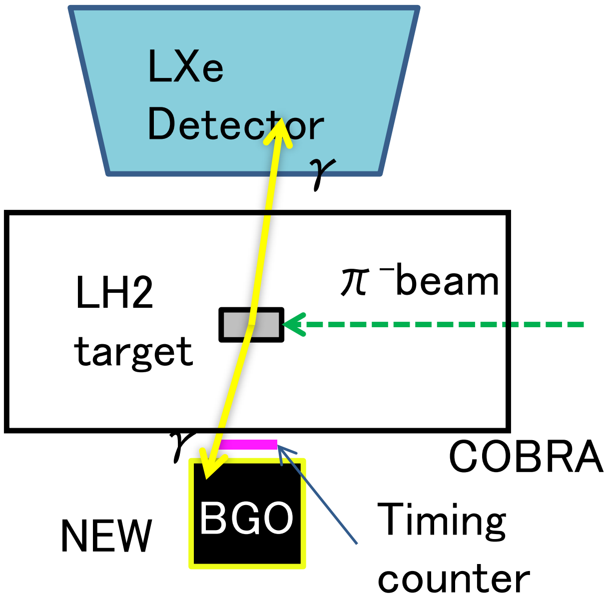

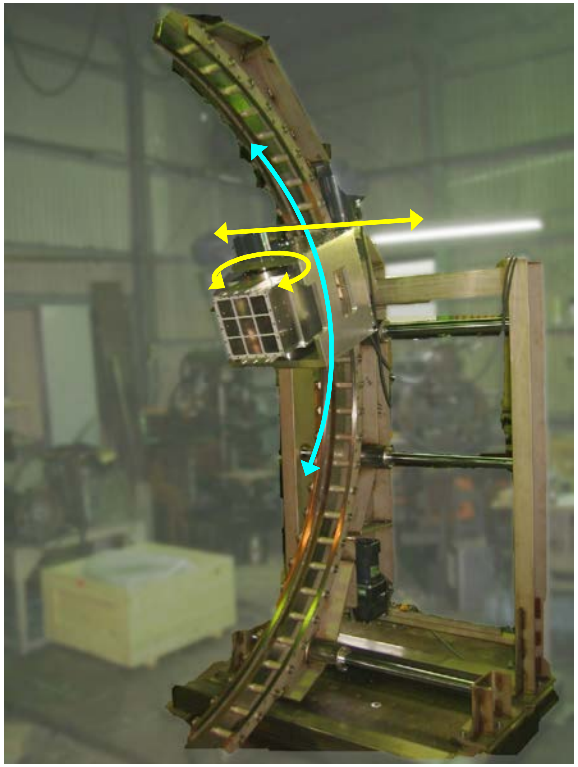

γ-ray resolutions

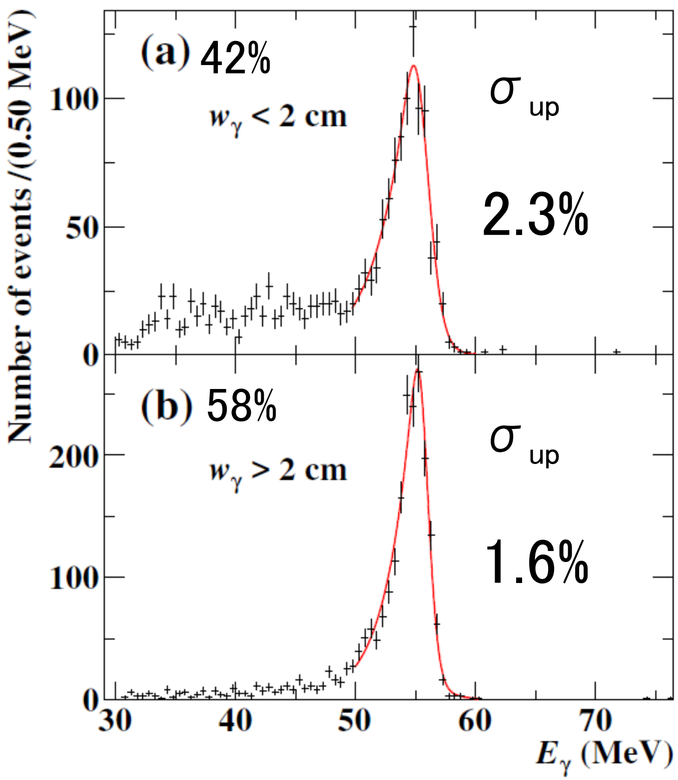

Fit 55MeV peak with response function considering

- Correlation of 2 γ angle and energy
- Difference of noise condition

Detector acceptance is divided into small parts and fit each.

When γ-ray convert at shallow part of the detector, energy resolution is worse

Position resolution is evaluated with lead collimator.
to be 5 mm σ in u, v direction and 6 mm σ in w direction.

COBRA magnet

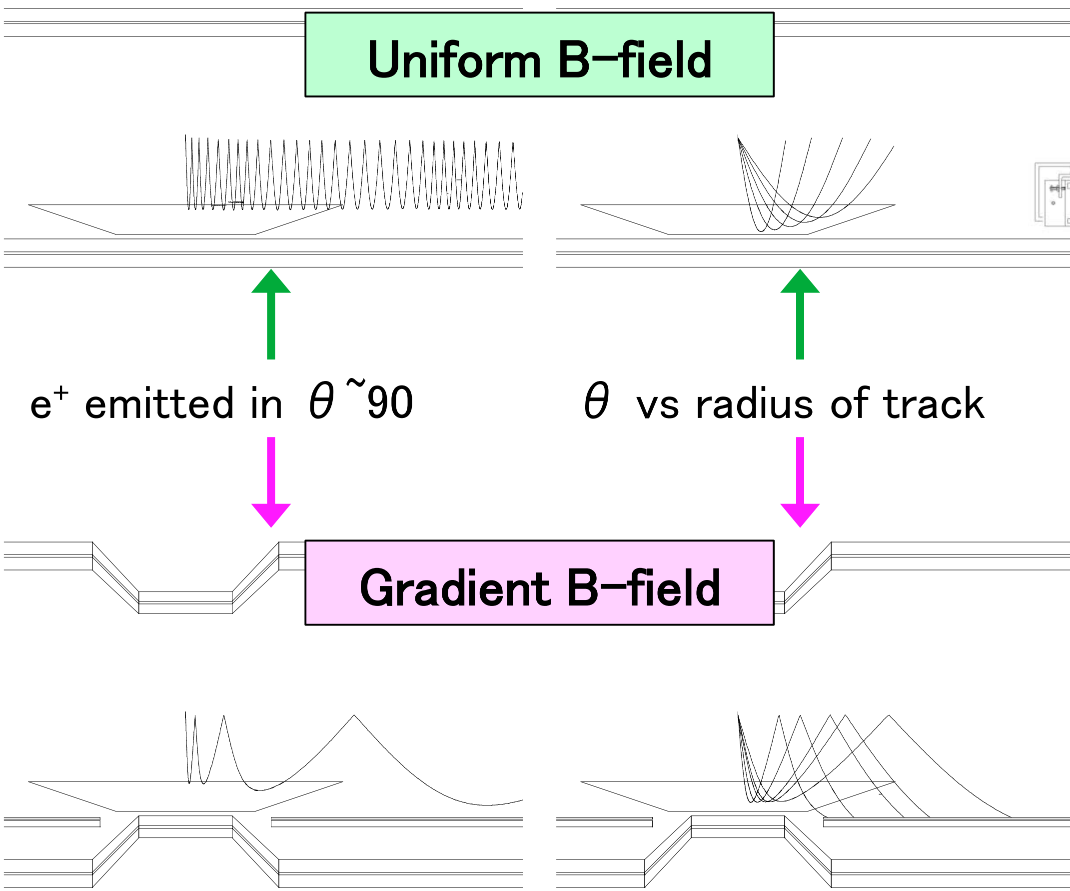

reduce pile up

low momentum e^+s are isolated

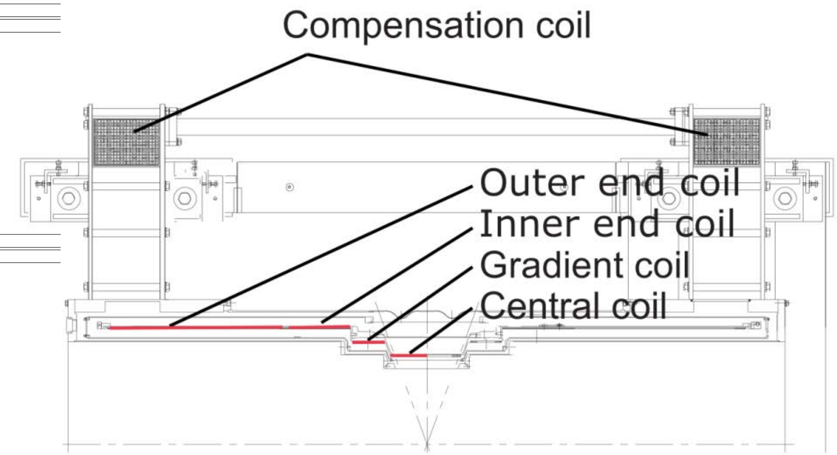

Characteristics

- Combination of SC magnets with different bore size
- Thin that γ-ray to transmit
- Cooled by GM refrigerator
- Compensation magnet which reduce field at LXe detector

Drift chamber
e^+ tracker

Interaction of e^+ and matter:

Multiple scattering → Worsens angular resolution
Pair annihilation → Generate γ-ray background

⇒ Low mass tracker

High-rate tolerance:

High rate μ^+s in beam eventually decay into e^+s.

⇒ 16 modularized detector in ϕ direction

Detector locate only at large R

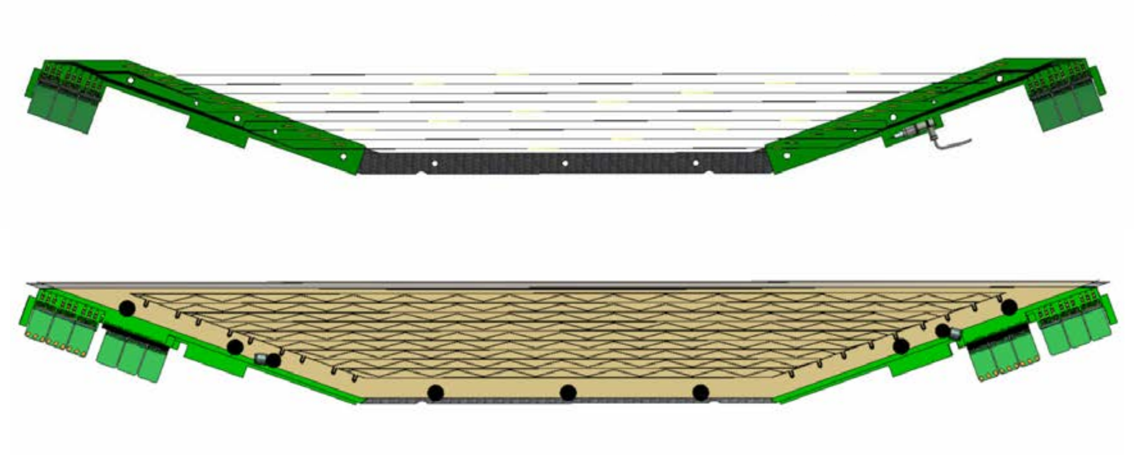

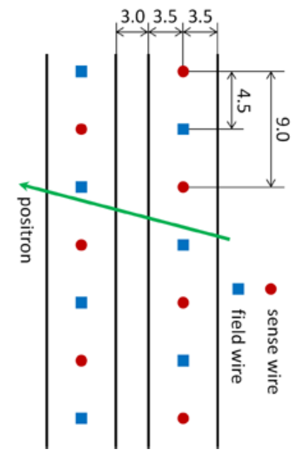

drift cell

e^+ track reconstruct

Hit detection by waveform analysis

↓

Reconstruct hit in each cell

- Ratio of charge on each side
- Detail z–position by vernier

↓

Connect neighboring hits

↓

First fit by circle

↓

Main fit of track

- Kalman Filter algorism is used

(Fit error in each event is utilized in final physics analysis)

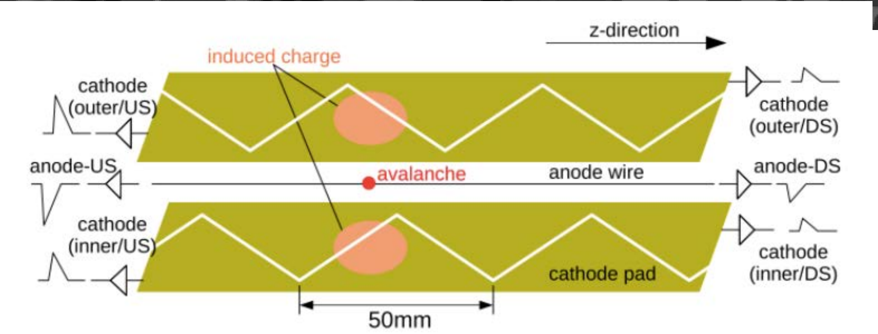

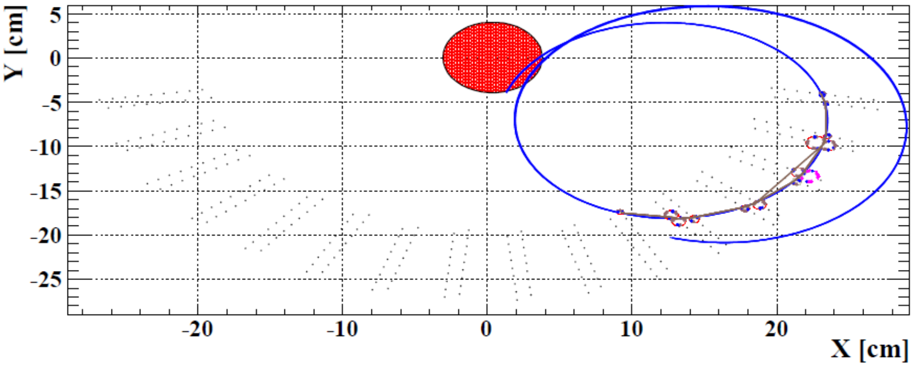

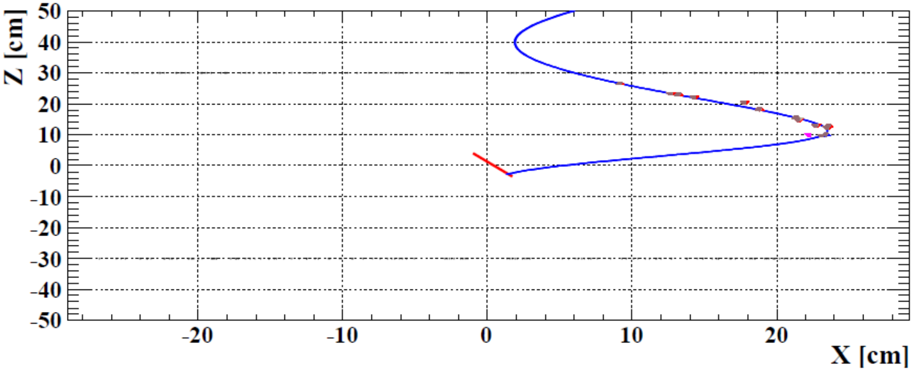

Positron observables

Positron energy resolution ($\sigma_{\mu e}$) is obtained by fitting spectrum of normal μ decay with response function.

① theoretical spectrum
② acceptance function
③ resolution function

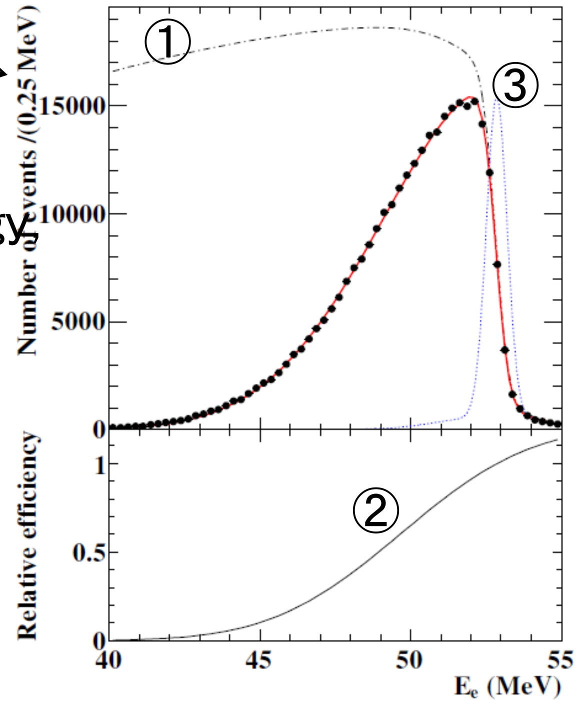

"Double turn" method is adopted to evaluate energy, position and angular resolutions.

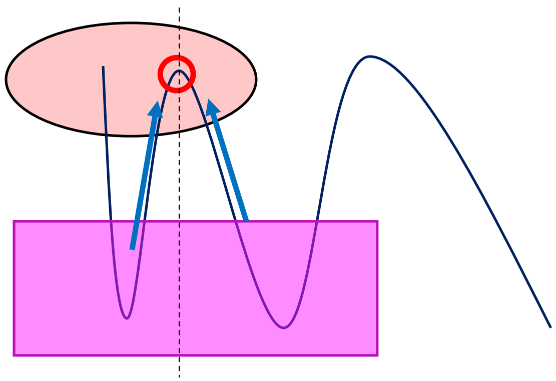

Independently propagate 1st and 2nd turn of genuine track.

Resolutions are largely affected by operation condition of DCH, but roughly
Ee ～ 300keV, θ e・ϕ e ～ 10mrad, ye ～ 1.3 mm, ze ～ 3.0mm

e+ timing counter

ϕ counter

- BC404 scintillator
  $4 \times 4 \times 79.6\ cm^3$
  15 bars on each side
- PMT read-out on both end
  (Fine mesh type)

z counter

- BCF-20 scintillation fiber
  Total 256 pcs.
- APD readout at one end

(※z counter is not used)

Assembled ϕ counter (one of two)

Roll of timing counter

- Precise measurement of e^+ hit time
- Provide information for trigger

Timing reconstruction

From the PMT hit time at TIC both end,
hit position and time at TIC bar is calculated.
Emission timing of positron needs track information (L_{track}).

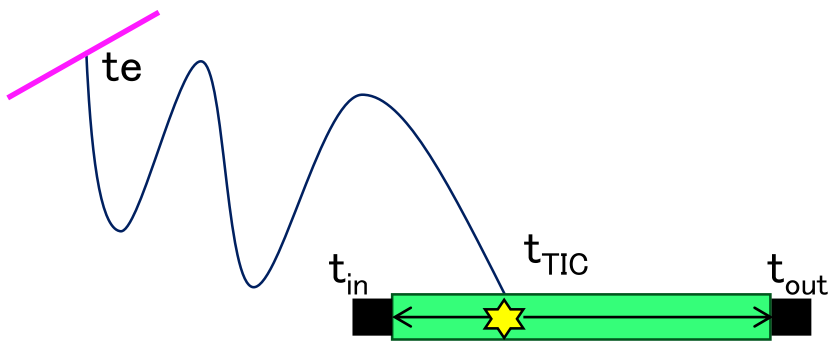

$$t_{\mathrm{TIC}} = \frac{t_{\mathrm{IN}} + t_{\mathrm{OUT}}}{2} - \frac{L_{\mathrm{bar}}}{2v}$$

$$z_{\mathrm{TIC}} = \frac{v}{2}(t_{\mathrm{IN}} - t_{\mathrm{OUT}})$$

Time-walk effect of PMT is corrected in t_{IN} , t_{OUT}.

Final timing observable is defined as,

$$t_{e\gamma} = \left(t_{\mathrm{LXe}} - \frac{|\boldsymbol{r}_{\gamma} - \boldsymbol{r}_{\mu}|}{c}\right) - \left(t_{TIC} - \frac{L_{\mathrm{track}}}{c}\right)$$

Timing resolution

Timing resolution is evaluated with RMD data, where all the γ-ray detector, positron detector, trigger are the same as the data for $\mu e \gamma$ physics data.
(Eγ, Ee correlation on teγ need to remove)

RMD events peak

Accidental

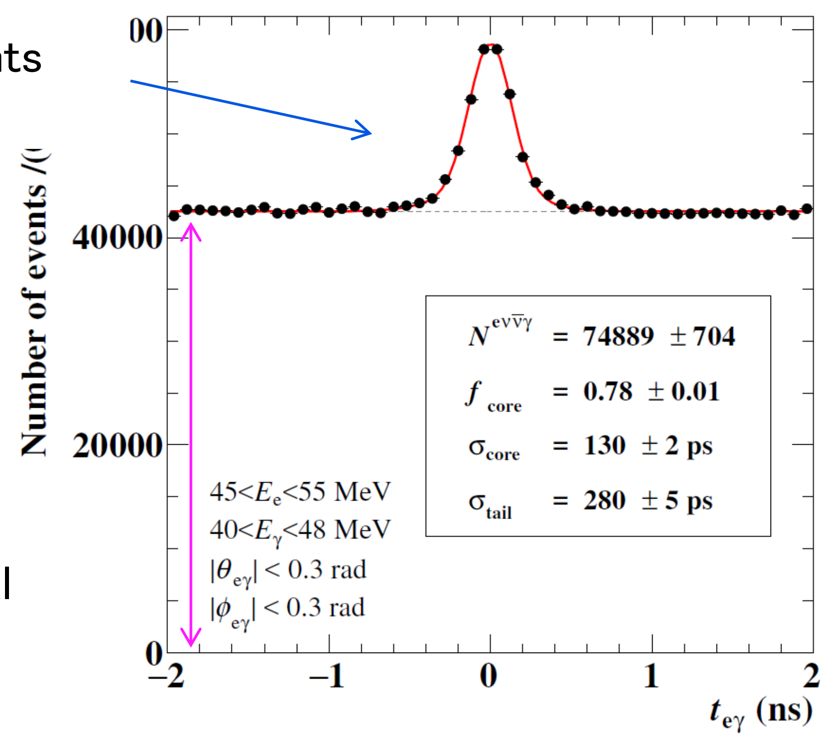

$\sigma_{e\gamma} = 122 \pm 4$ ps

resolutions
for each component
$\sigma t\gamma$ ~ 65 ps
σte ~ 100 ps

Efficiencies

γ-ray detection efficiency

62.5±2.3%, for γ from target aiming at detector acceptance

Loss: material between (COBRA, cryostat wall, PMT etc)

leakage of electro-magnetic shower

positron detection efficiency

48% from Monte Carlo simulation.

※It is not needed in physcis analysis

Trigger efficiency

After improvement in 2011

trigger rate13Hz

Live Time ratio 99%

Selection efficiency 97%

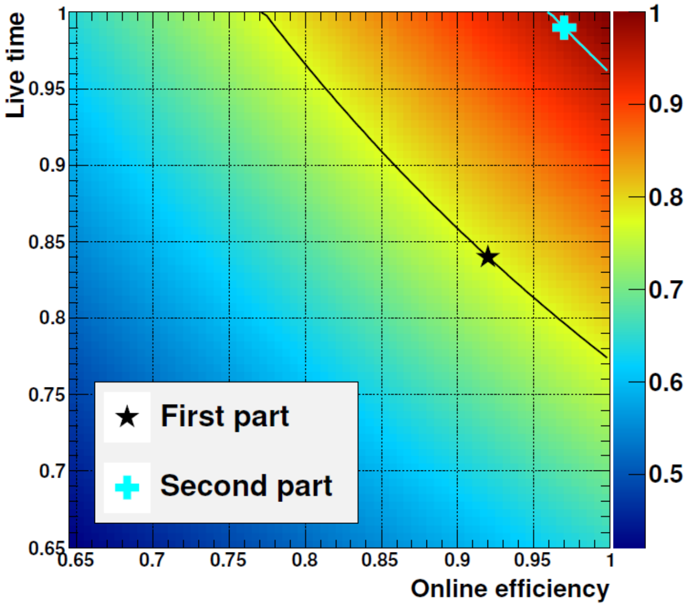

3. Analysis and Result

History of MEG

2000 2004 2008 2012 2016

design construction data taking

1999
PSI proposal
Approval

2007
Detector
Complete

2010
Nucl. Phys. B
834 1

2.8 x 10^{-11}
(90%CL)

2011
Phys. Rev. Lett.
107, 171801

2.4 x 10^{-12}
(90%CL)

2013
Phys. Rev. Lett.
110, 201801

5.7 x 10^{-13}
(90%CL)

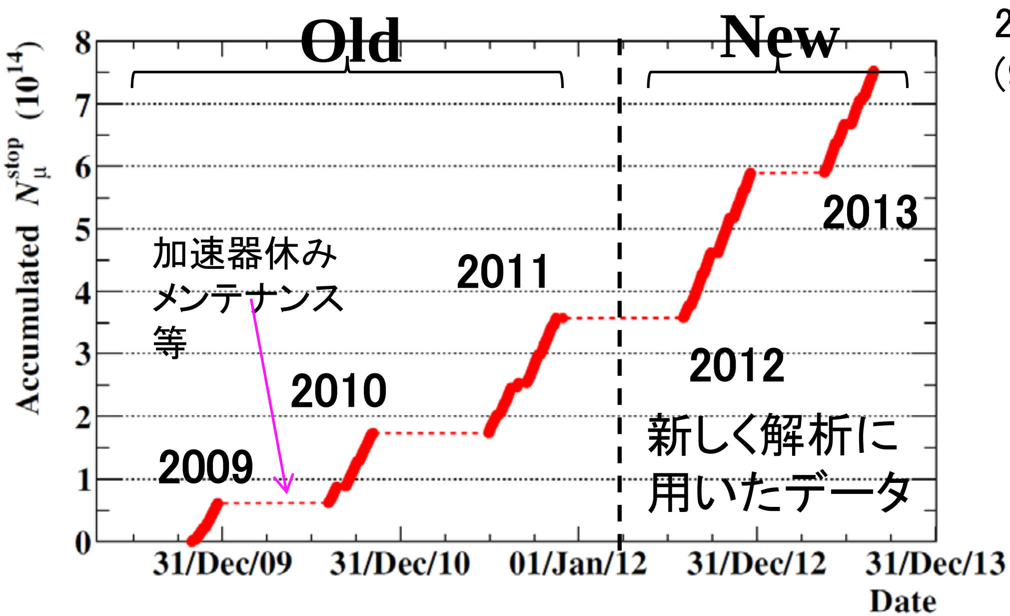

通算データ量 93 TB
通算DAQ時間 288日
通算run数 124156
(~2000 event/run)
通算静止μ^+数 7.5×10^{14}

Event selection

Firstly, apply pre-selection in order to obviously accidental events.

Then, detailed calibration is done on passed events

Final event selection is defined as,

$48 < E\gamma < 58$ MeV
$50 < Ee < 56$ MeV
$|te\gamma| < 0.7$ ns
$|\theta e\gamma| < 50$ mrad
$|\phi e\gamma| < 75$ mrad

Region $|te\gamma| < 1.0$ ns is blinded at first.
Parameter for physics analysis is determined by outside (sideband) events.

Signal events will concentrate around here, if exist.

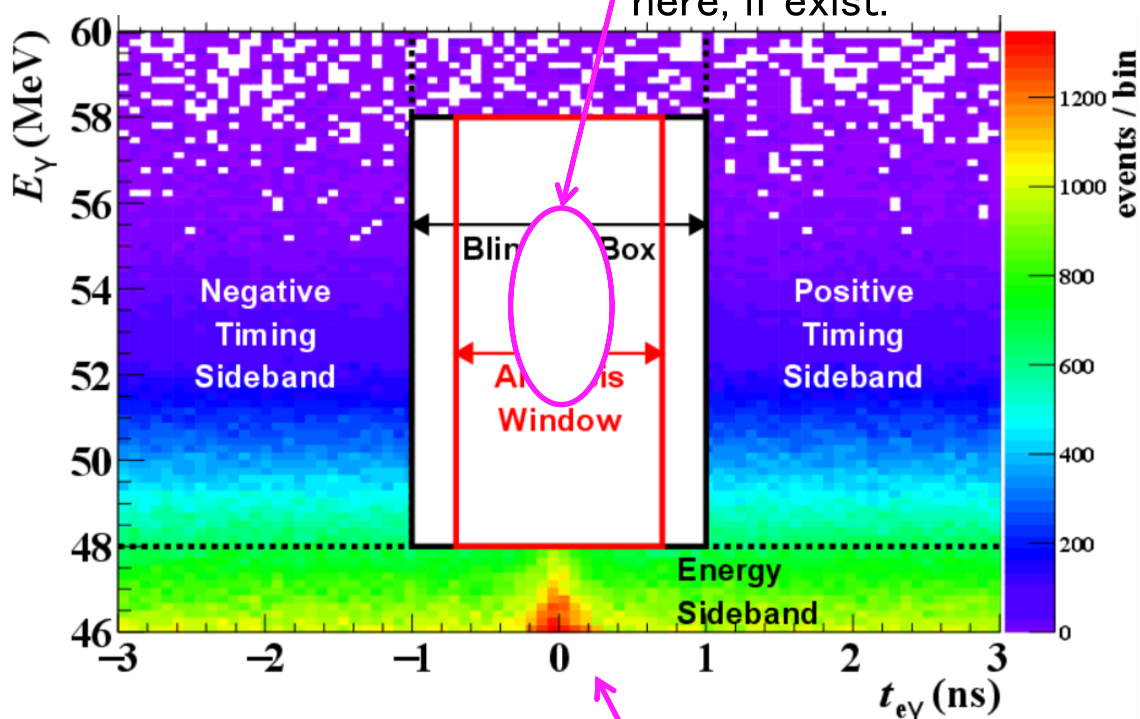

RMD

Likelihood analysis

Definition of MEG likelihood function

extended likelihood — constraint term

$$\mathcal{L}(N_{\mathrm{sig}}, N_{\mathrm{RMD}}, N_{\mathrm{ACC}}, \vec{t}) = \frac{e^{-N}}{N_{\mathrm{obs}}!} C(N_{RMD}, N_{ACC}, \vec{t})$$

$$\times \prod_{i=1}^{N_{\mathrm{obs}}} (N_{\mathrm{sig}} S(\vec{x_i}, \vec{t}) + N_{\mathrm{RMD}} R(\vec{x_i}) + N_{\mathrm{ACC}} A(\vec{x_i}))$$

PDF

$\boldsymbol{N = N_{sig} + N_{\mathrm{RMD}} + N_{\mathrm{ACC}}}$

$\vec{\boldsymbol{t}}$: Target parameter

$\boldsymbol{N_{\mathrm{obs}}}$: Event number in window

$\vec{\boldsymbol{x}}$: $(\boldsymbol{E_\gamma, E_e, t_{e\gamma}, \theta_{e\gamma}, \phi_{e\gamma}})$

$\boldsymbol{S, R, A}$: (Probability Density Function)

$\boldsymbol{C}$: Constrain N_{RMD} N_{ACC} around expectation in side band

Best fit value is defined by such that maximized likelihood function
Confidence interval is determined with Feldman-Cousins approach, setting Nsig as the main parameter, and profiling out the others.

PDF

Probability to find the observable to be the value when Signal, RMD, AccBG happens.

Determined from sideband data (partially Monte Carlo simulation)

All known correlations between observables,
detector position etc. are corrected.

event-by-event PDF
- Shape of function changes, according to
  - Error in reconstruction
  - Position in detector
  - Correlation

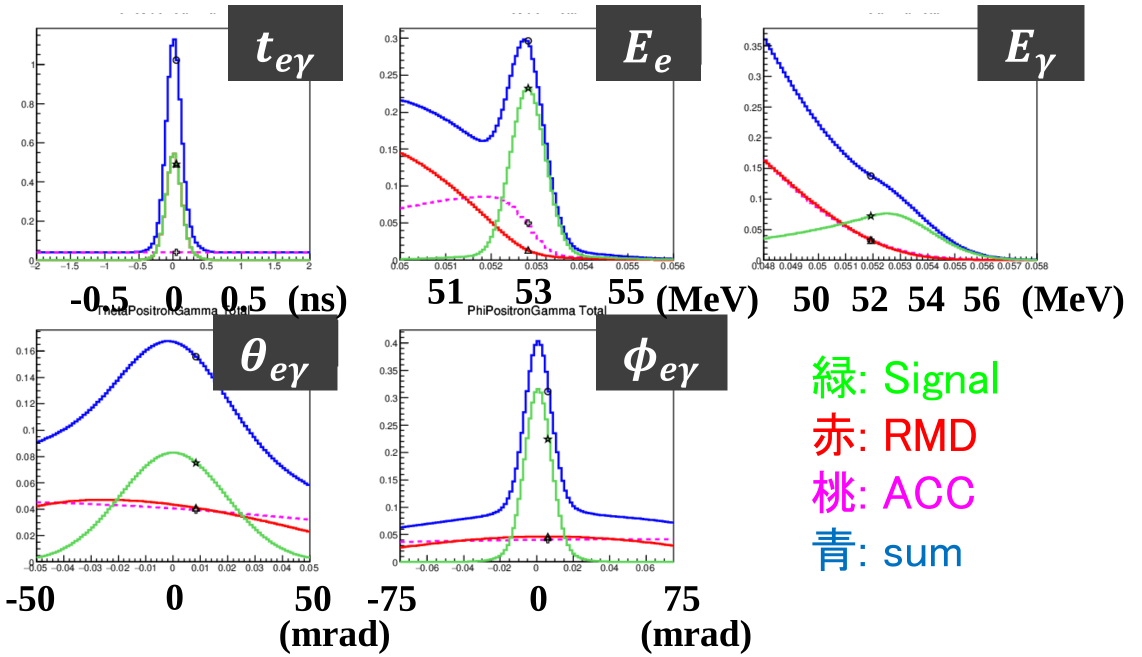

Examples in certain events

Target Position

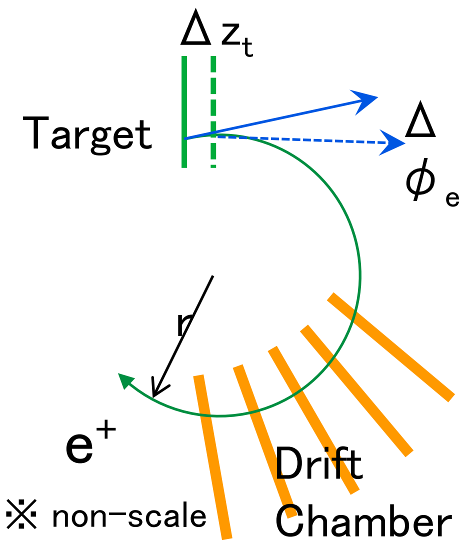

There are 2 methods

1. Optical method → next page
2. Software method

   Utilize correlation of apparent hole position depends on position direction.

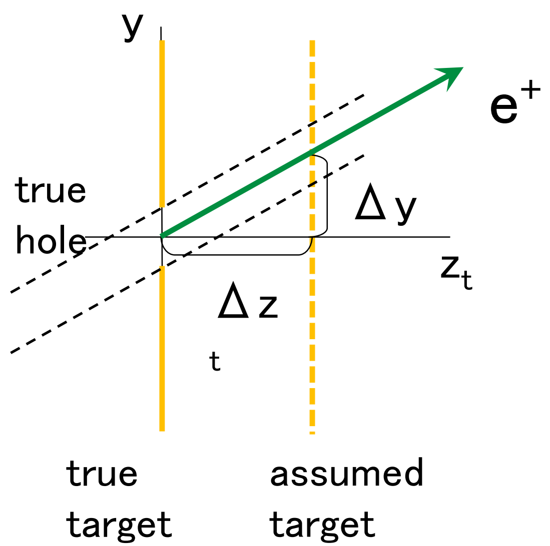

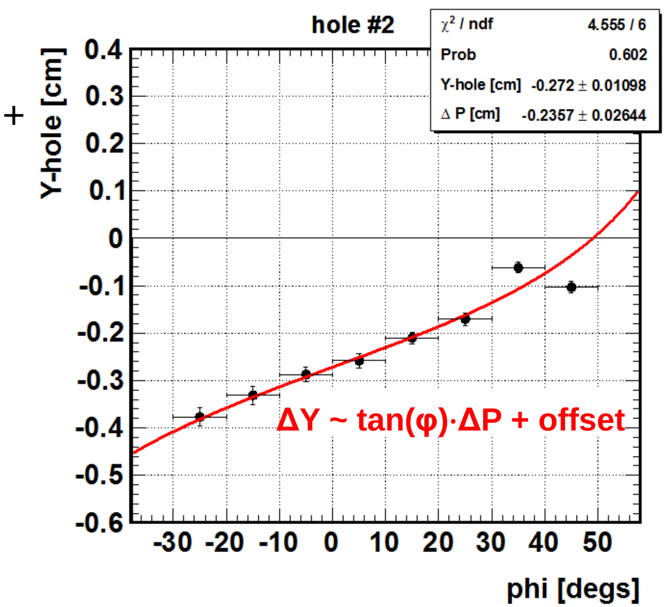

When
$r \sim 10$ cm
$\Delta z_t \sim 1$ mm,

$\Delta \phi e \sim 10$ mrad
(ϕe reso. 10mrad)

Target measure

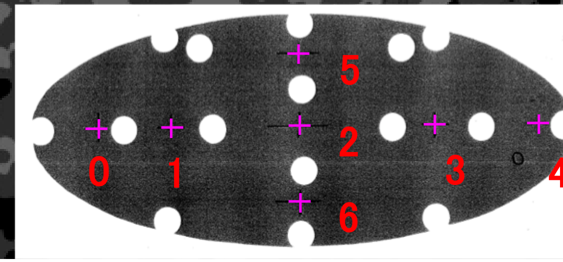

Measure target with theodolite.
Conventionally fit is done with plane, but expanded to paraboloid fit.

2009–2011 data can be seen as plane, but
2012, 2013 data has large strain.

Cross marker
Plane fit
Paraboloid fit
Hole position

Horizonal

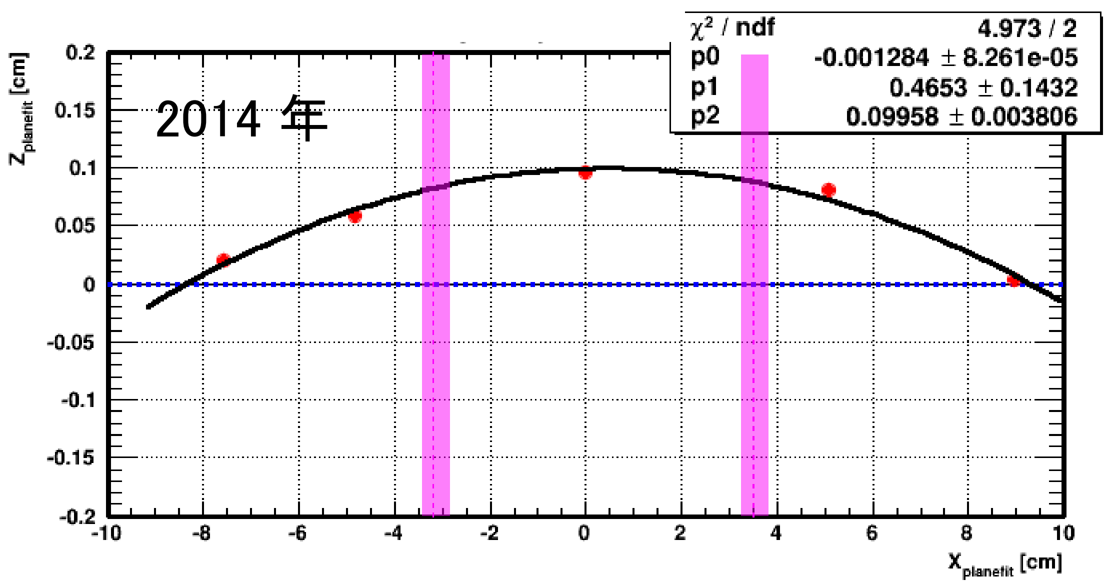

Vertical

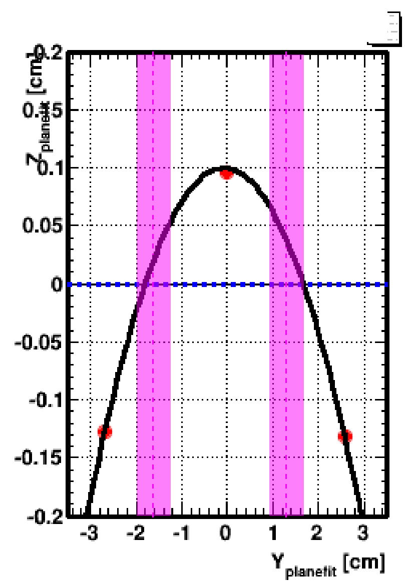

Deformation & countermeasure

For detail investigation 3D laser scan was performed in 2015.

As the result, deformation of complex shape was found, but around the beam-spot, paraboloid is a good approximation.

Countermeasure :

1. In trac reconstruction, set start point of e^+ (= μ stopped point) to be fitted paraboloid。 (previously fitted plane)

2. Remaining uncertainties = position・local shape are taken into account as nuisance parameters.

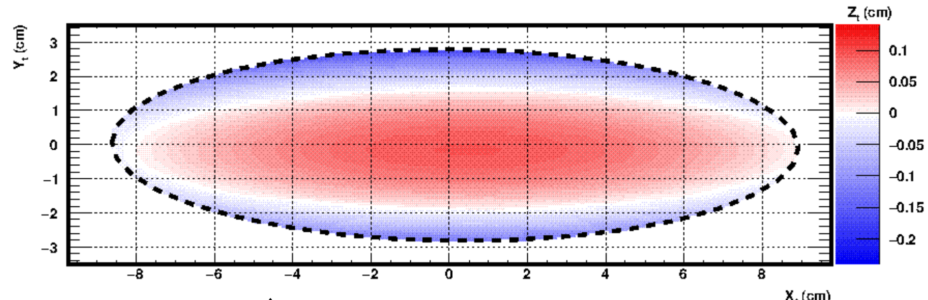

↑ 2013 paraboloid

↓ Result of 3D scan

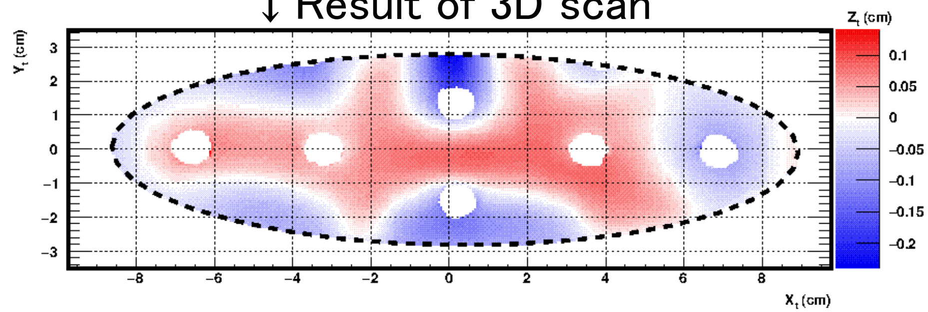

Target uncertainty

Shift center of $\phi_{e\gamma}$ PDF for Signal event PDF.

$$\Delta\mu_{\phi} = \underbrace{\Delta_{\mu}\phi_{e\gamma}(p,\phi_{e})}_{\text{Parallel shift}} + s\underbrace{[\Delta_{\mathrm{FARO}}\phi_{e\gamma}(x_{e},y_{e}) - \Delta_{\mathrm{para}}\phi_{e\gamma}(x_{e},y_{e})]}_{\text{Paraboloid of 3D scan}}$$

p : Parallel shift parameter

s : Local shape parameter

0 ～ 1

Paraboloid ～ 3D scan

p and *s* are independent for each year,

Δ_{FARO} is scaled to match with curvature of paraboloid fit.

p is constrained by Gaussian dist. centered at 0 (error 300 (500) um)

s is constrained in [0,1] for 2013, narrower region for previous years.

Impact on sensitivity :

Sensitivity is worsened by13% in sensitivity.

This is largest systematics, and the others occupy only 1%.

positron AIF recognition (Annihilation in Flight)

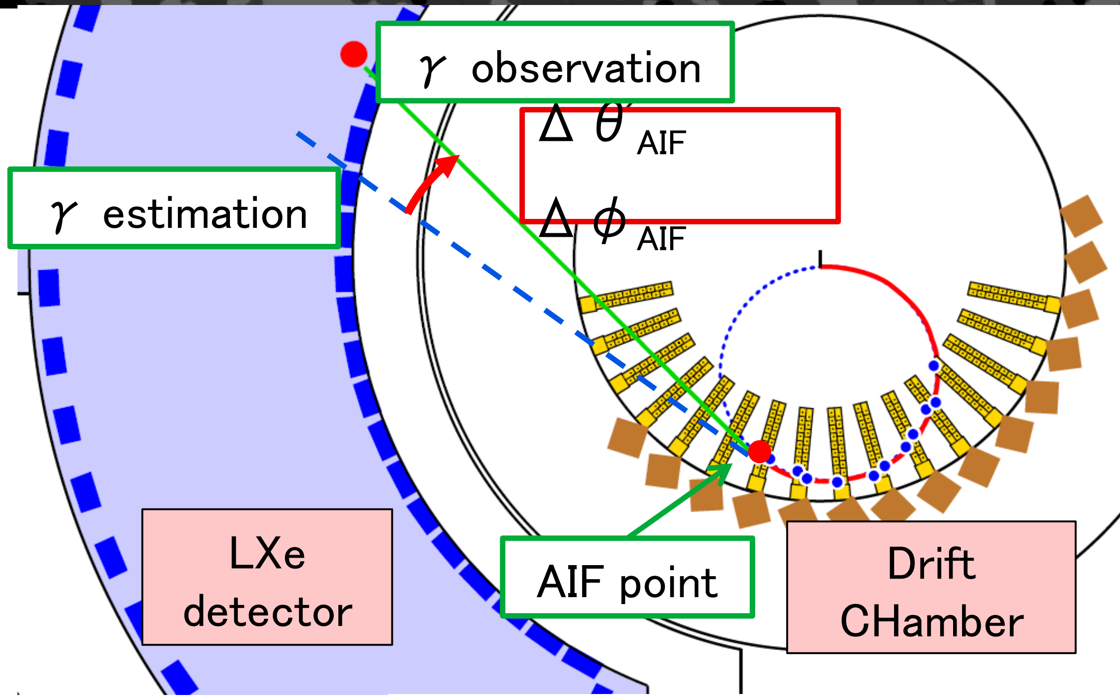

Tag one of the sources of γ-ray, "positron AIF"

A. Recognize interrupted e^+ track in drift chamber
B. Estimate γ-ray momentum from that before AIF
C. Calculate angle difference between estimation and observation

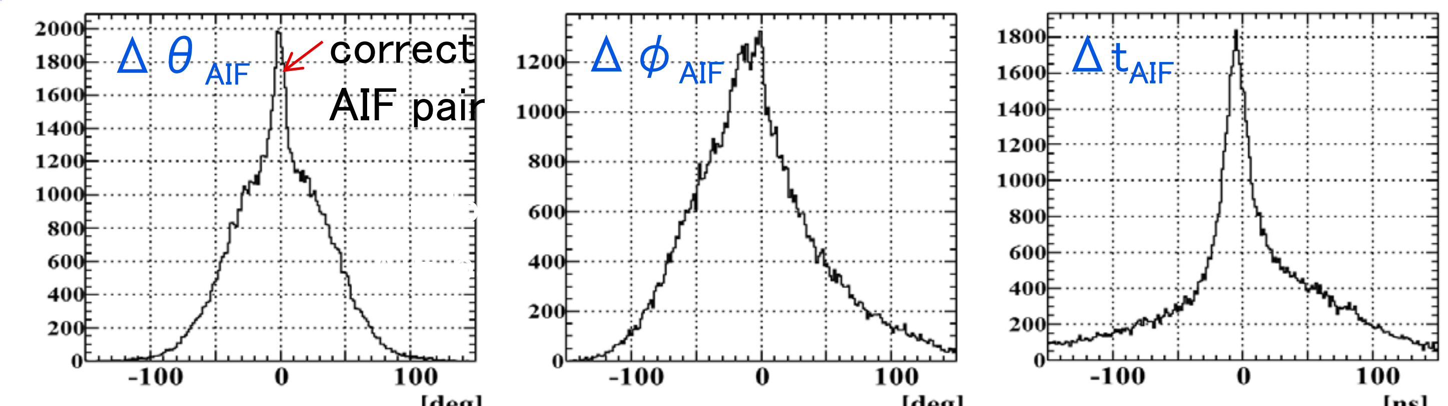

AIF reduction and impact

Sharp peak in $\Delta\theta_{AIF}$, $\Delta\phi_{AIF}$ distribution is really tagged AIF events.
Cut events near peak.
※Precise shape of Δt_{AIF} distribution is difficult to obtain.
It is used only for rough cut.

Method :

1. Fit 2D distribution $\Delta\theta_{AIF}$, $\Delta\phi_{AIF}$ with combination of 2D Gaussian function. (2 peak and 1 base component.)

2. Remove events within 0.7σ from either of the peaks, as they are likely to be AIF Accidental BG.

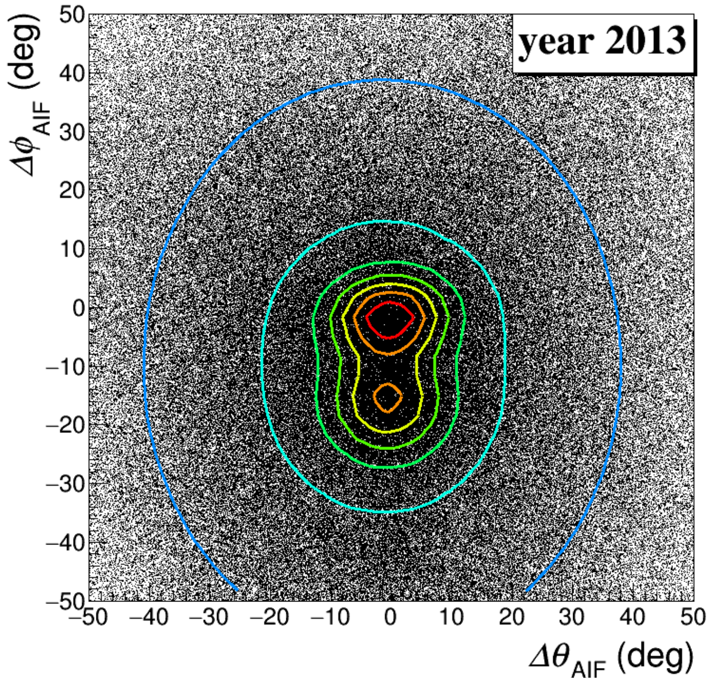

Impact :

No significant improvement in sensitivity.
Insurance for AIF event to come near center of window.

Normalization

A constant to convert event number and $\mu^+ \to e^+ \gamma$ branching ratio

$$\mathcal{B}(\mu^+ \to e^+\gamma) = \frac{\Gamma(\mu^+ \to e^+\gamma)}{\Gamma_{\mathrm{TOTAL}}} = \frac{N_{\mathrm{sig}}}{k}$$

Norm. factor

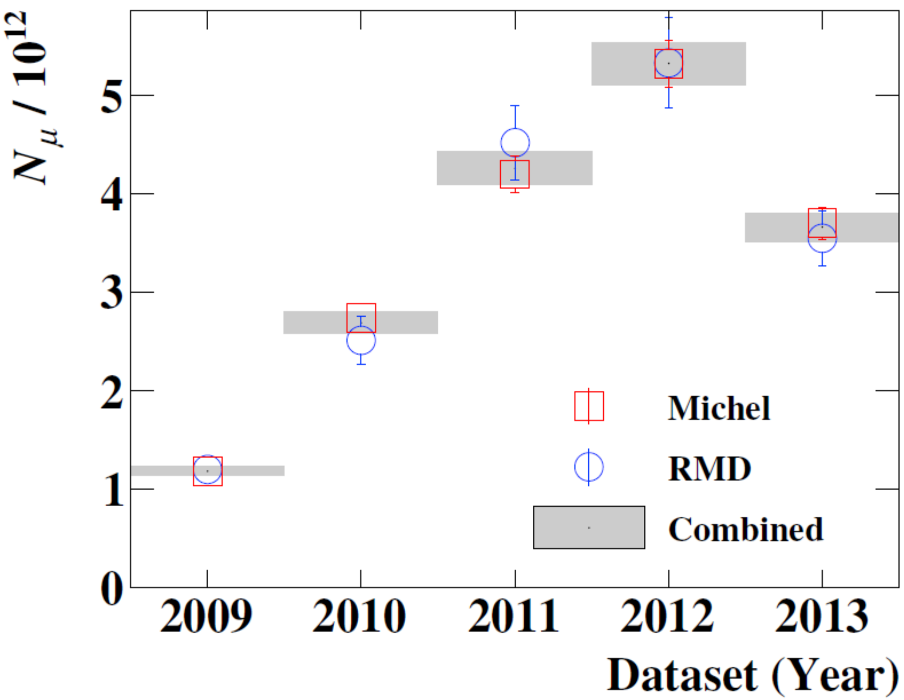

k is considered to be a number of events multiplied with detector acceptance and detection efficiency,

There are independent 2 ways,
Michel positron way and RMD way.
Final value is given by combining two.

Both ways do not need e^+ detection efficiency.

For all statistics of MEG data,

$k = 1.71 \pm 0.06 \times 10^{13}$

Search sensitivtiy

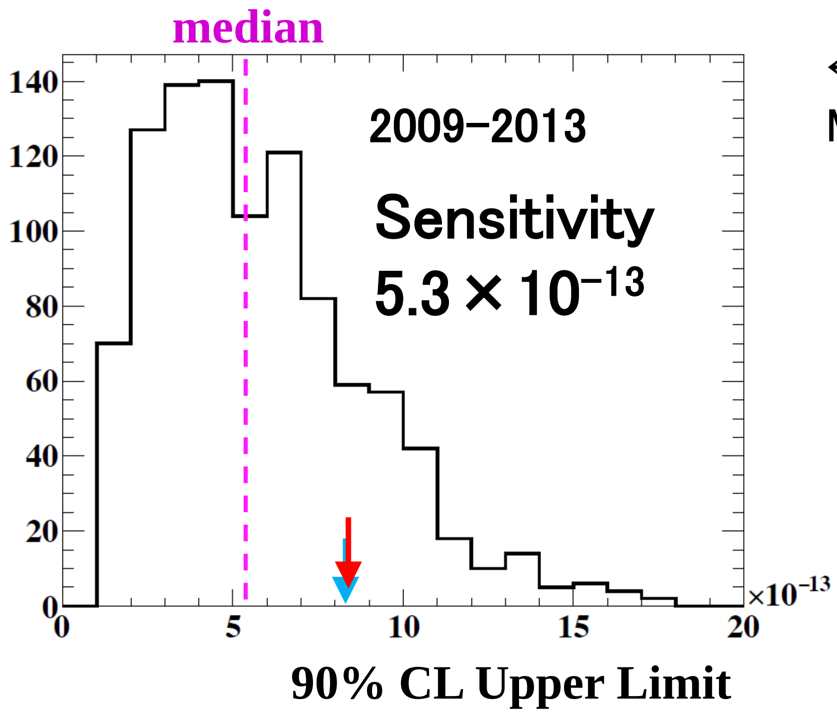

←Histogram of upper limits of many Toy MCs which do not contain signal.

Data set	2009–2011	2012–2013	2009–2013
k (× 10^{12})	8.15	8.95	17.1
Sensitivity (× 10^{-13})	8.0	8.2	5.3

(90% CL)

Arrows are limit from time sideband (−2.0ns, +2.0ns)
8.4×10^{-13}, 8.3×10^{-13}

Previous publication(2009–2011)
Sensitivity was 7.7×10^{-13}
Understandable, considering the changes in analysis.

Event distribution

2009-2013
full data

Excess of the signal is not seen.

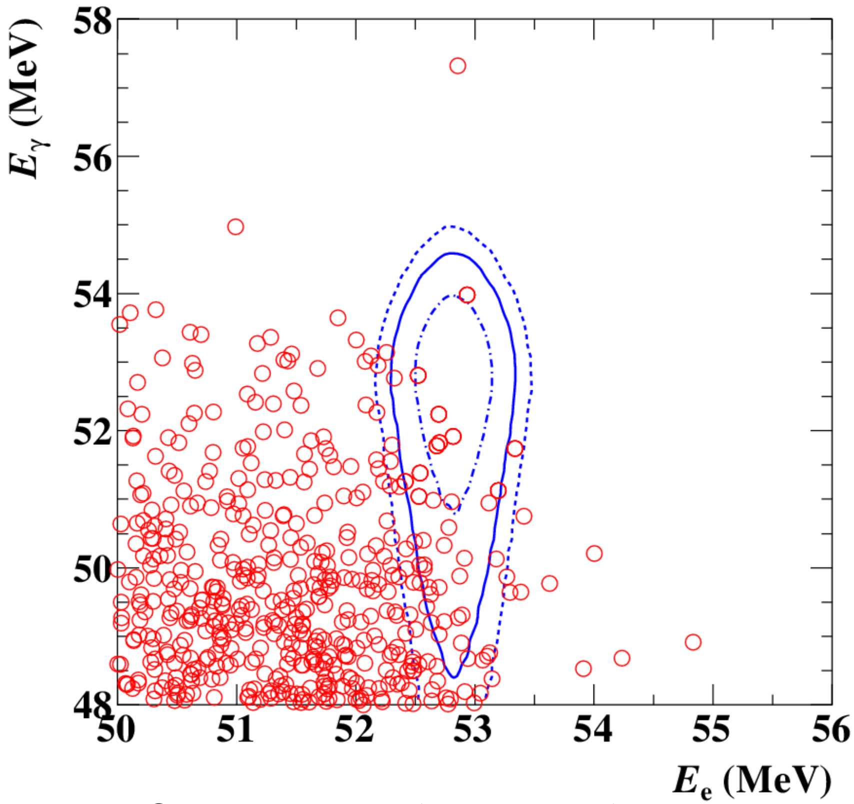

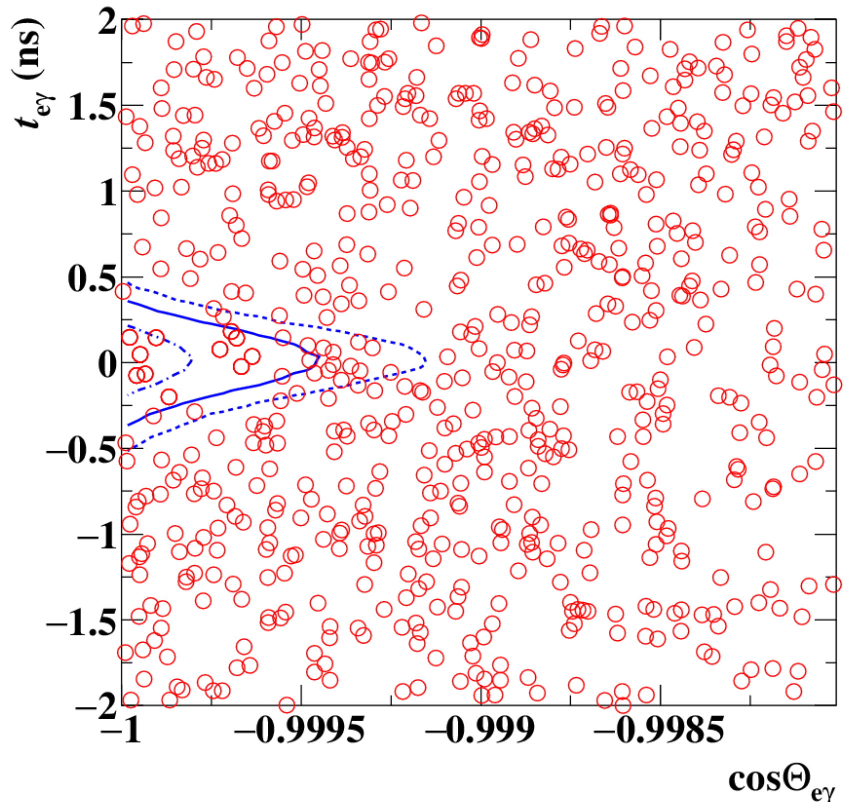

$\cos\Theta < -0.99963$ (90% ε_{signal})
$|t_{e\gamma}| < 0.2443$ns (90% ε_{signal})

$51 < E_\gamma < 55.5$ MeV (74% ε_{signal})
$52.385 < E_e < 55$ MeV (90% ε_{signal})

Contours show averaged signal PDF (1σ, 1.64σ, 2σ)

Fit result

← 2009–2013 full data

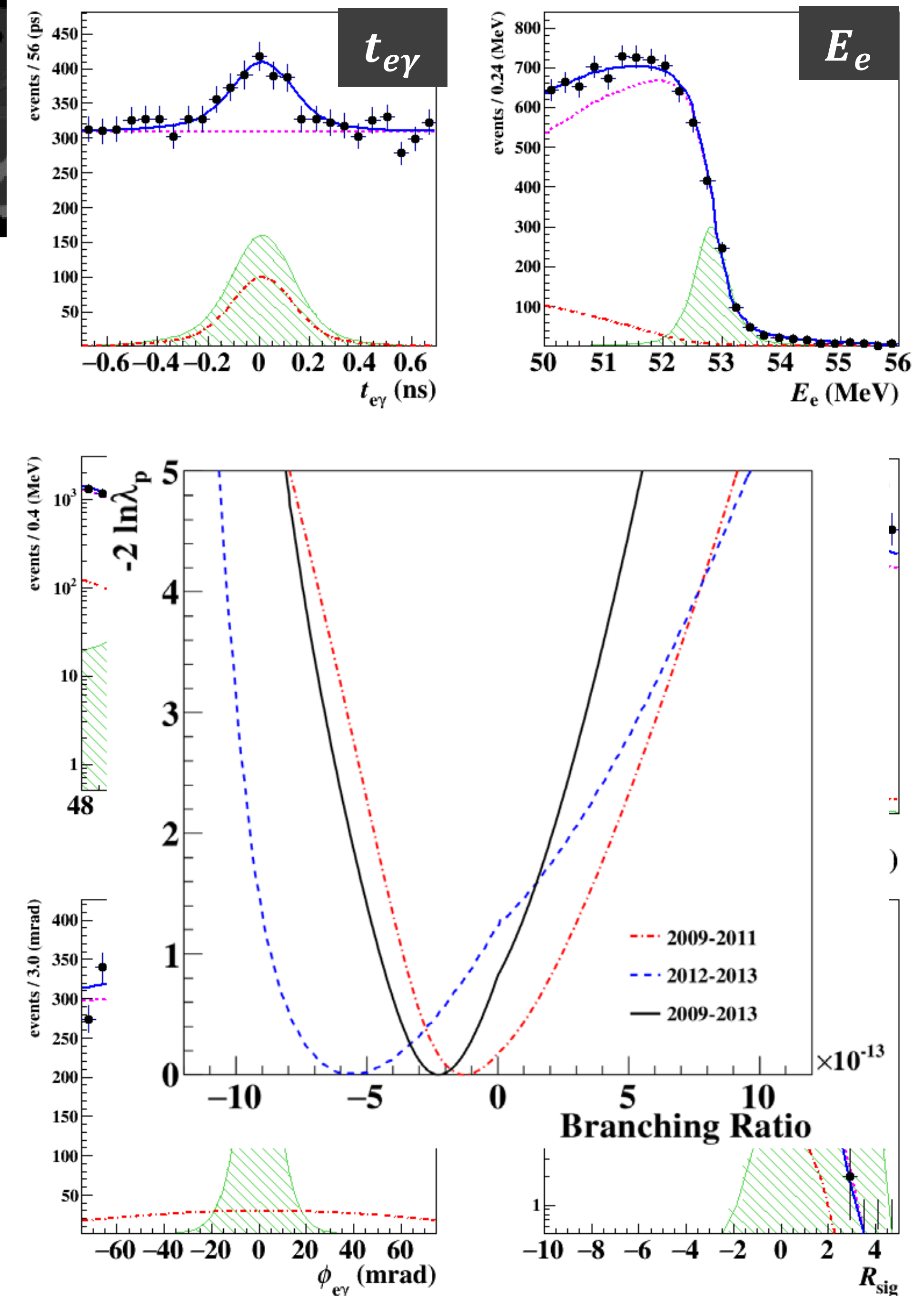

● data
ACC
signal (500events)
sum
RMD

Data and projected PDF agree well.

Data set	2009–2011	2012–2013	**2009–2013**
best fit $\mathcal{B}$ ($\times 10^{-13}$)	−1.3	−5.5	**−2.2**

←Indication for signal-likelihood Rsig

$$R_{\text{sig}} = \frac{S(\overrightarrow{x_i})}{0.07R(\overrightarrow{x_i}) + 0.93A(\overrightarrow{x_i})}$$

Confidence interval

Consistent with no signal assumption

Data set	2009–2011	2012–2013	2009–2013
$\mathcal{B}$ 90% UL (×10^{-13})	6.1	7.9	4.2
Sensitivity (×10^{-13})	8.0	8.2	5.3

In previous result, 5.7×10^{-13} with 2009–2011 data.
Consistent including change in analysis.

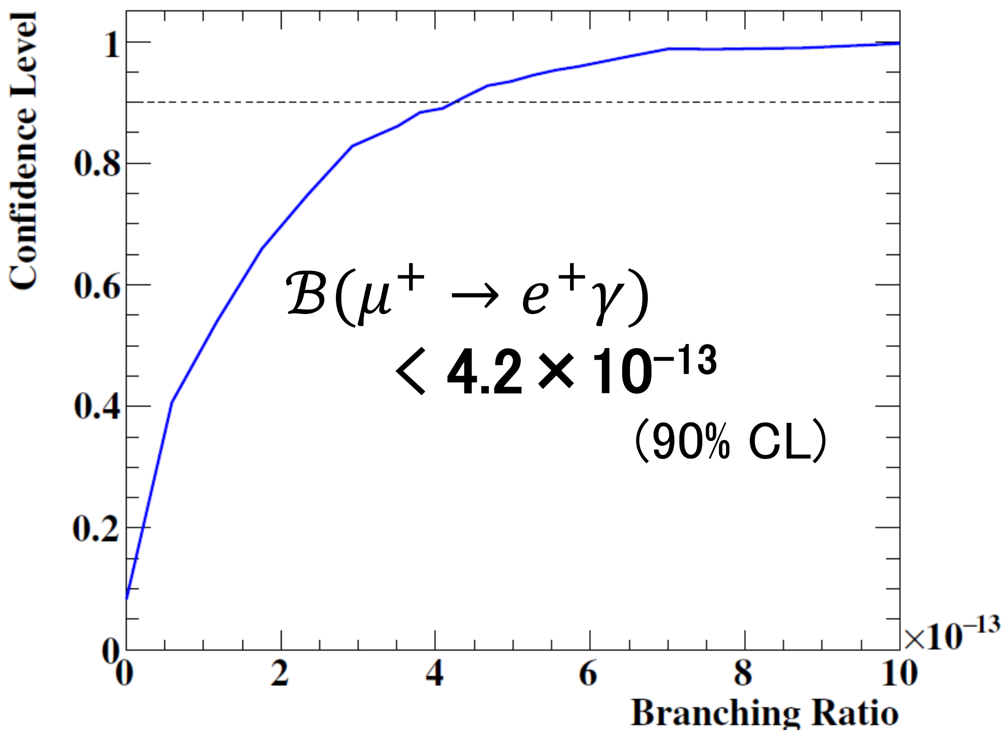

CL curve with 2009–2013 data
(Ratio of ToyMC with $\lambda_p^{\mathrm{MC}} < \lambda_p^{\mathrm{data}}$)

Move of the observables

High rank event in either (current/previous) of results are plotted.

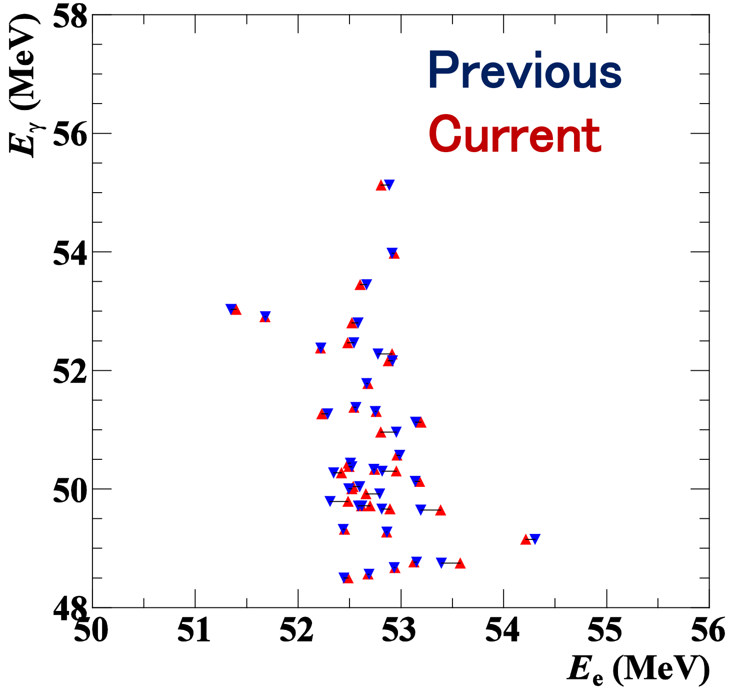

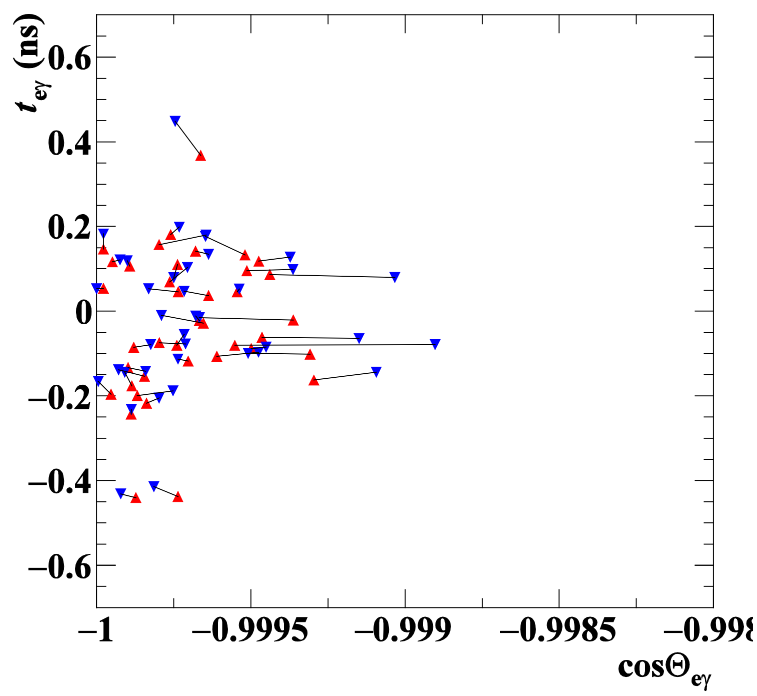

We tested MC experiment to simulate move of observables and compared upper-limits.
Data located around the center of the MC distribution.

Fit result constrain

Usual likelihood function contains constraint term for N_{RMD} と N_{ACC} to be near to the estimation from sideband.

$$C\left(N_{\mathrm{RMD}}, N_{\mathrm{ACC}}, \vec{t}\right) = \exp\left\{-\frac{(N_{\mathrm{RMD}} - \mu_{\mathrm{RMD}})^2}{2\sigma_{\mathrm{RMD}}^2}\right\} \exp\left\{-\frac{(N_{\mathrm{ACC}} - \mu_{\mathrm{ACC}})^2}{2\sigma_{\mathrm{ACC}}^2}\right\} c(\vec{t})$$

In order check the BG distribution in analysis window, fit without constrain term were tested.

		2009 –2013	
N_{ACC}	expect	7743.7	±41.2
	fit no constr.	7684.4	±103
	standard fit	7739.1	±37.7
N_{RMD}	expect	614.4	±33.8
	fit no constr.	663.3	±59.1
	standard fit	624.6	±28.4

4. MEG II experiment

MEG II experiment

Upgrade aiming at 10 times higher sensitivity of MEG

Main features

- 2.3 times stronger beam
- target not easy to deform
- Replace PMT of inner face of LXe with MPPC
- Unified, larger volume, stereo wired drift chamber
- Pixelated timing counter with SiPM read out
- New detector to tag RMD AccBG

Expected sensitivity is 4×10^{-14}

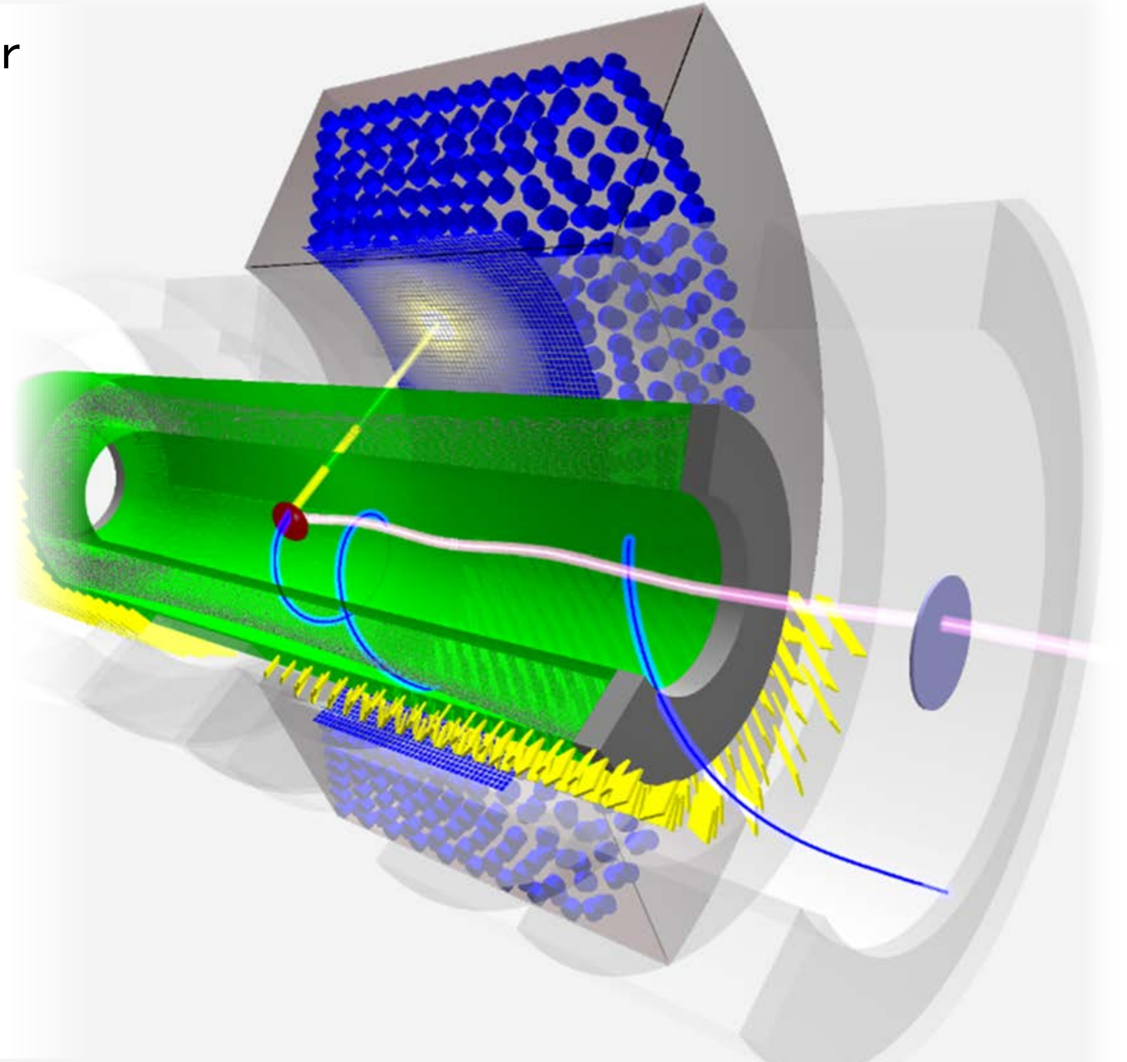

MEG II status

Xenon detector

Drift chamber

Timing counter

RDC counter

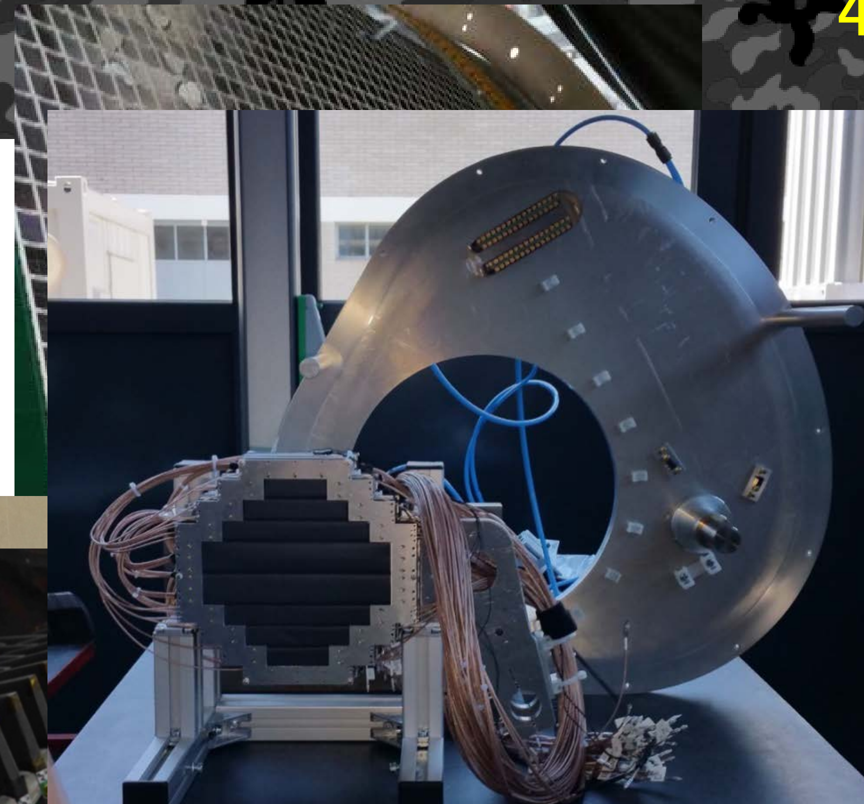

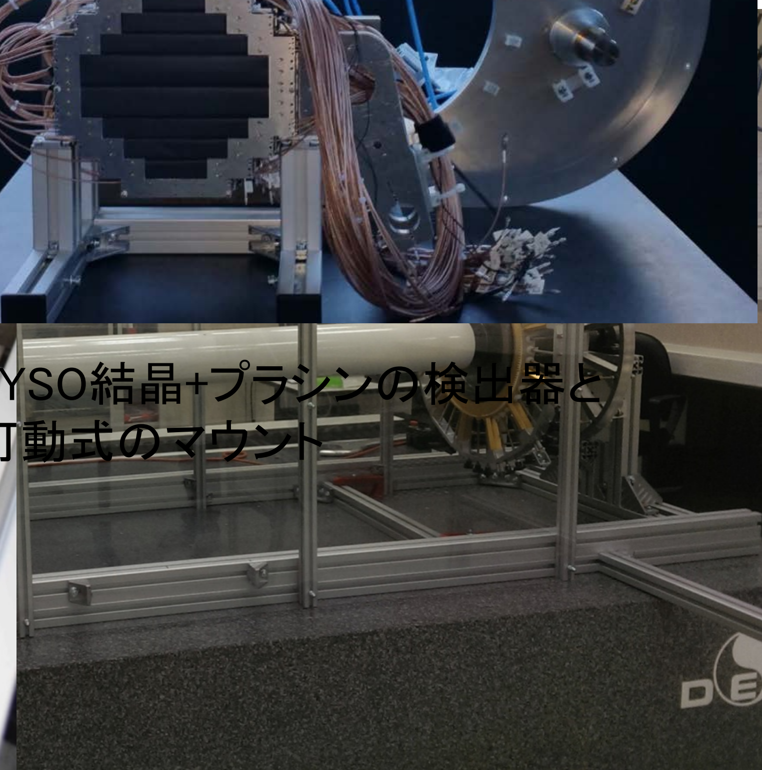

LYSO結晶+プラシンの検出器と
可動式のマウント

MEG II prospects

Specification	MEG I	MEG II
Beam intensiy (/s)	3×10^7	7×10^7
Resolutions		
E γ (%, w>2 / w<2)	2.4/1.7	1.1/1.0
γ pos. (mm, u/v/w)	5/5/6	2.6/2.2/5
Ee (keV)	306	130
θ e γ / ϕ e γ (mrad)	9.4/8.7	5.3/3.7
te γ (ps)	122	84
Efficirncies (%)		
trigger	>99	>99
γ	63	69
e^+	40	88

R&D

←2012

2013 Upgrade proposal approve

assembly

←2016

2017 upgrade complete
start data taking

DAQ

3 years

sensitivity
4×10^{-14}

←2020

Summary

MEG experiment is searching for $\mu^+ \to e^+ \gamma$, evidence of the physics beyond the standard model of particle.

MEG I experiment has been finished and we published final result **Eur. Phys. J. C, 76(8), 1–30**
New limit 4.2×10^{-13} is 30 times more stringent than MEGA experiment.

MEG II experiment is aiming

おわり

近縁のCLFV探索

◎ μ−e 転換（$N\,\mu^- \to N\,e^-$）

現在の上限値はSINDRUM−II実験から $B<7\times10^{-13}$ (N=Au)

新しい実験の準備が進んでいる

COMET, DeeMe, Mu2e

◎ μ→eee 崩壊

PSIにて、Mu3e実験が準備中

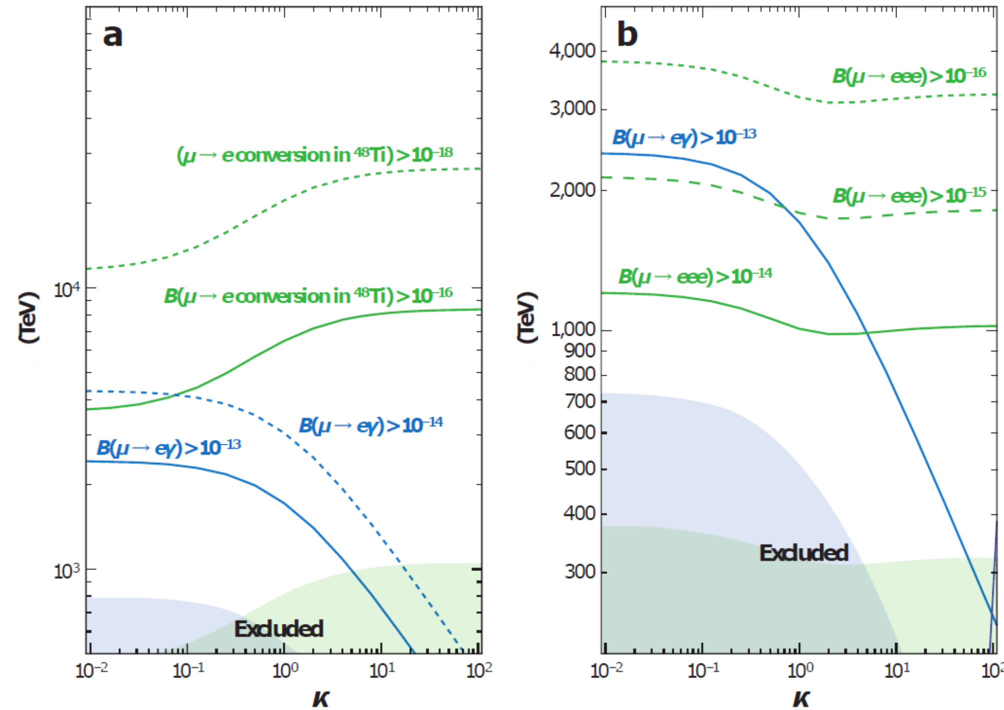

これら2つのチャンネルは、
μeγとは異なるタイプの
相互作用も可能で
μeγと相補的関係にある。

$$\mathcal{L} = \frac{m_\mu}{(\kappa+1)\Lambda^2}\bar{\mu}_R\sigma_{\mu\nu}e_L F^{\mu\nu} + \frac{\kappa}{(1+\kappa)\Lambda^2}\bar{\mu}_L\gamma_\mu e_L(\bar{f}_L\gamma^\mu f_L)$$

μeγと共通

μeγには無い項

キセノン補助システム

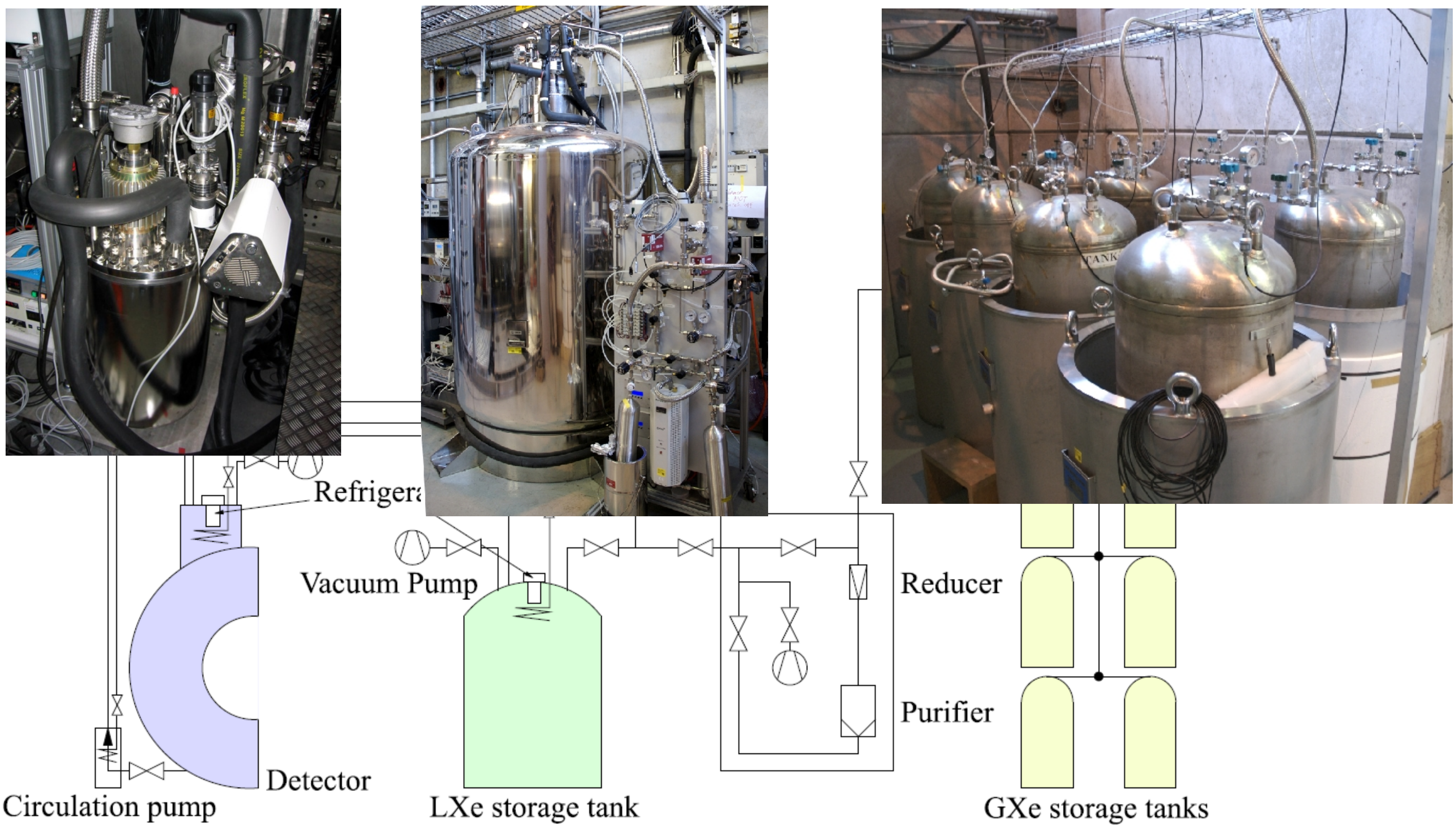
Refrigera
Vacuum Pump
Reducer
Purifier
Detector
Circulation pump
LXe storage tank
GXe storage tanks

エレクトロニクス

典型的な
エレキチェーン

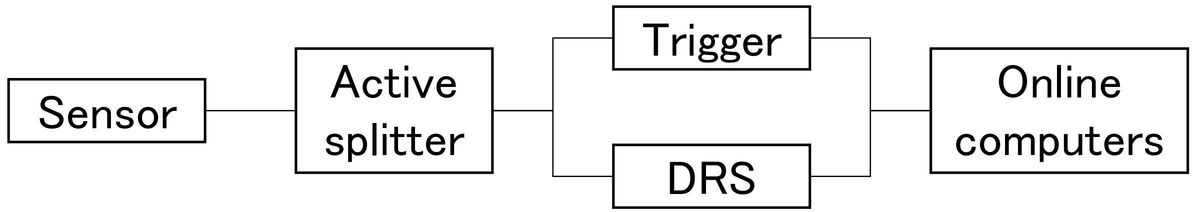

data size
～1 MB/event
(compressed)

Trigger :
 FPGAを用いて高速な事象再構成を行い、
トリガー情報を作る。
条件: γ線エネルギー
γ−e⁺の時間差 trigger rate
γ−e⁺の方向 ～13 Hz

DRS :
PSIで開発された波形取得装置
サンプル速度 1.4GHz (DCHは0.7GHz)

MIDASシステム採用 :
データの取得・スローコントロール
を管理するシステム。PSIが開発。

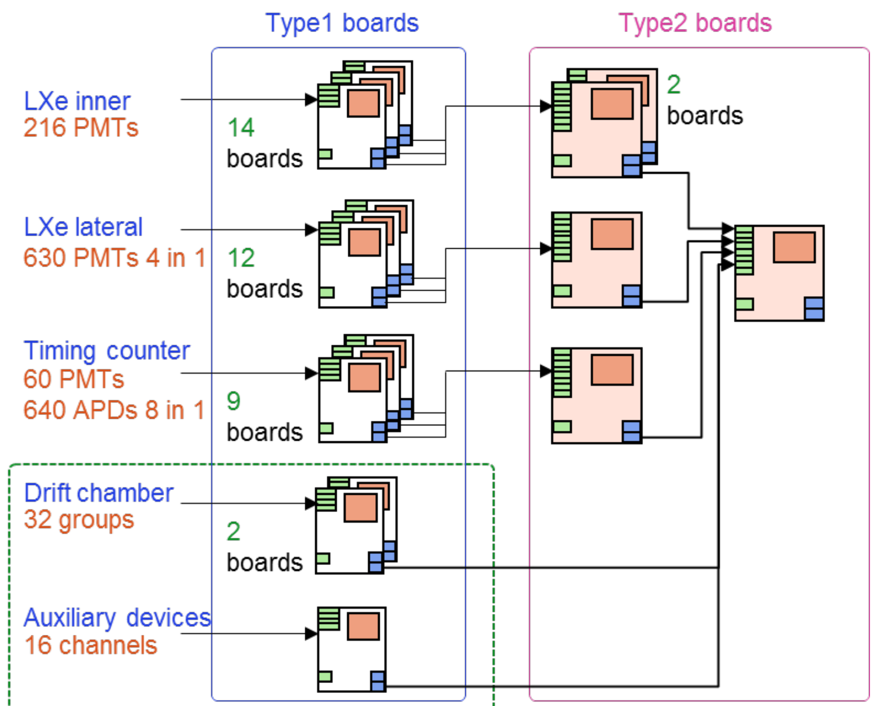

トリガーシステムの構成

事象再構成:概要

再構成でのデータの流れ

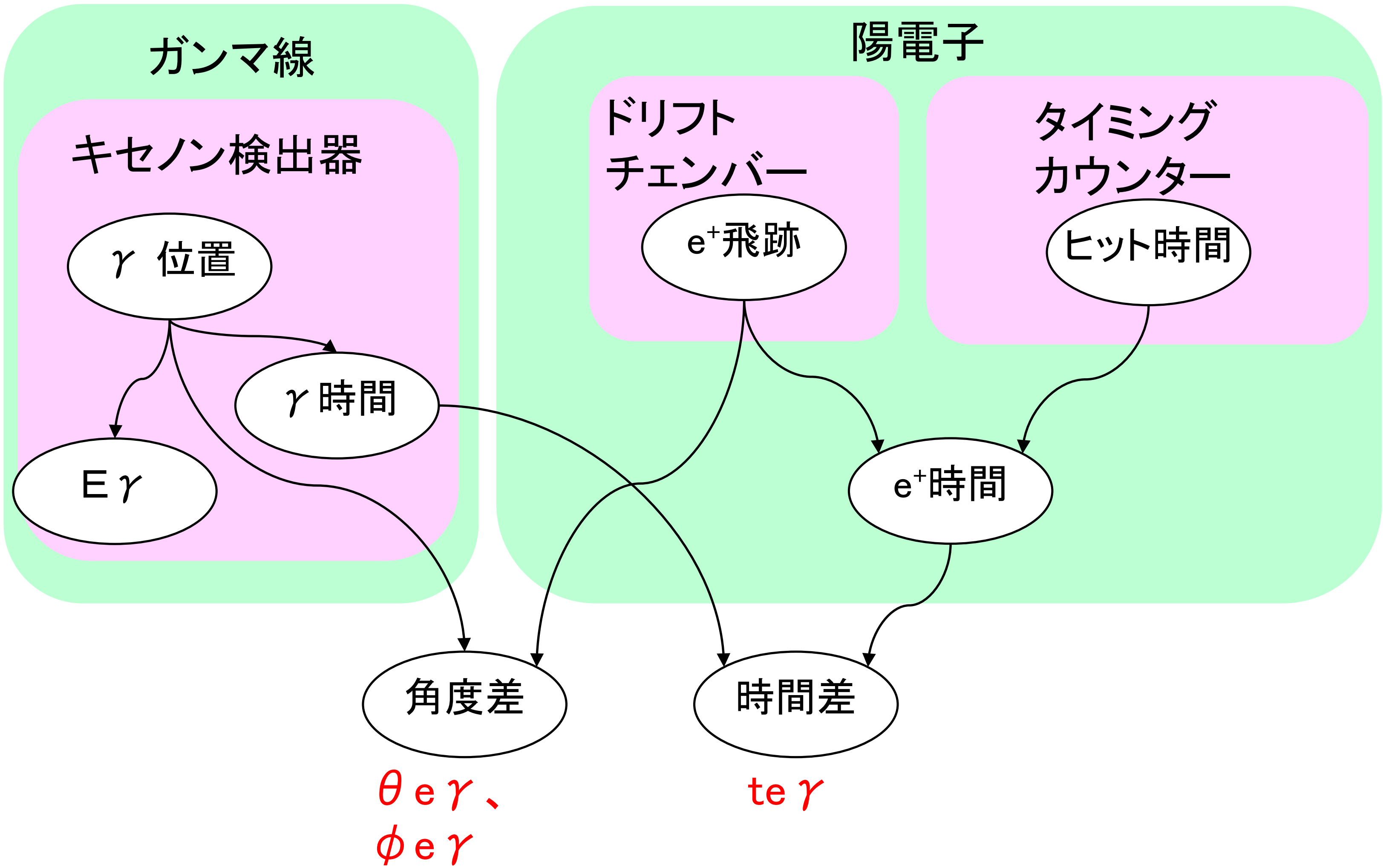

γ線 位置・時間

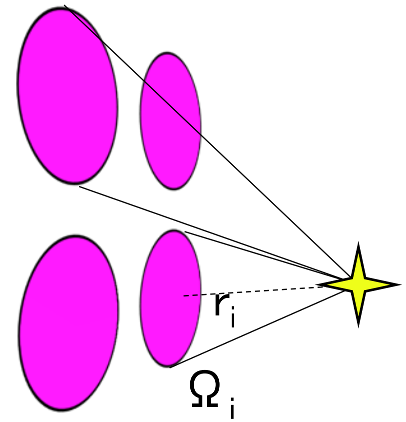

位置 (キセノン中で最初に反応した点)

a. 中心付近の光子数の分布をχ^2フィット

b. フィット結果の補正
シャワーの大きさ・斜め入射

1点から等方的にシンチレーション光が放たれていると仮定。

$$\chi^2_{\mathrm{pos}} = \sum_i \left(\frac{N_{\mathrm{pho},i} - c\Omega_i(u,v,w)}{\sigma_{pho}\left(N_{\mathrm{pho},i}\right)} \right)^2$$

時間(キセノン中で最初に反応した時間)

$$\chi^2_{\mathrm{time}} = \sum_i \left(\frac{t_{\mathrm{PMT},i} - \frac{r_i}{v} - t_{\mathrm{LXe}}}{\sigma_t\left(N_{\mathrm{phe},i}\right)} \right)^2$$

– 和は50光電子以上のPMTについてとる

γ線 エネルギー

エネルギー

各PMTの波形の和から計算される。

- PMTごとの光子の伝搬時間は差し引いておく。
- それぞれのPMTの重みは次を考慮する。

  - PMTのゲインと量子効率（光電子の収集率も含む）
  - PMTがカバーする立体角
  - 面ごとの補正係数
  - 放出点から光電面を見込む立体角
  - γの位置による不均一性の補正

sum波形

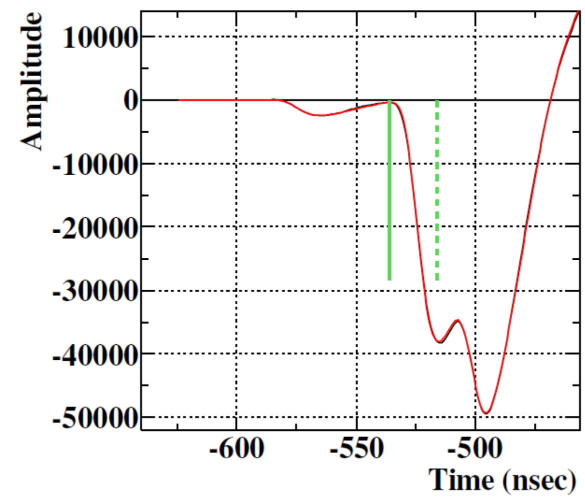

pile-up unfolding

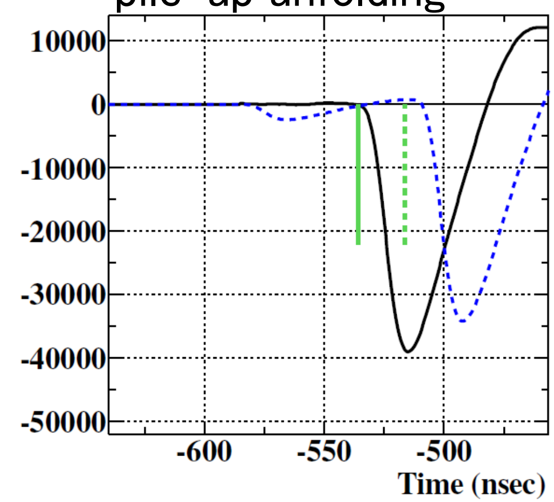

複数γ線のパイルアップへの対処

- シンチレーション光の空間分布
- sum波形のピークサーチ

ミッシングターン復元

陽電子がチェンバーを複数回通過する場合、
それぞれの周回が別の陽電子として識別されてしまう事があった。
一つの陽電子による分かれた軌跡を識別し復元する手法を導入した。

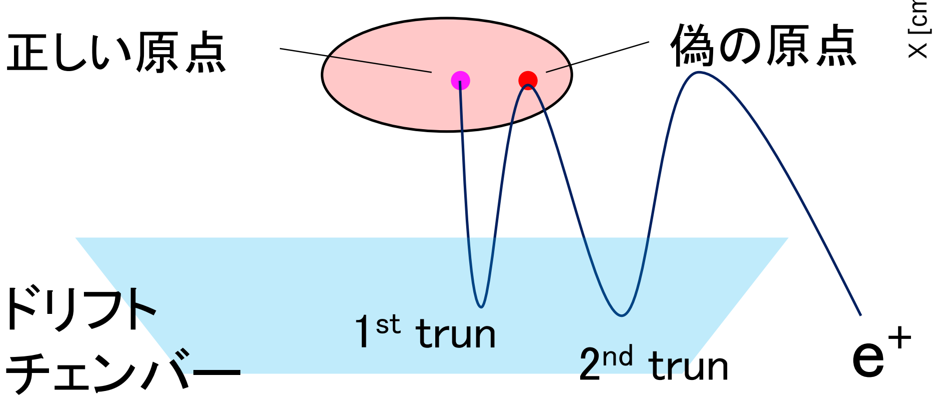

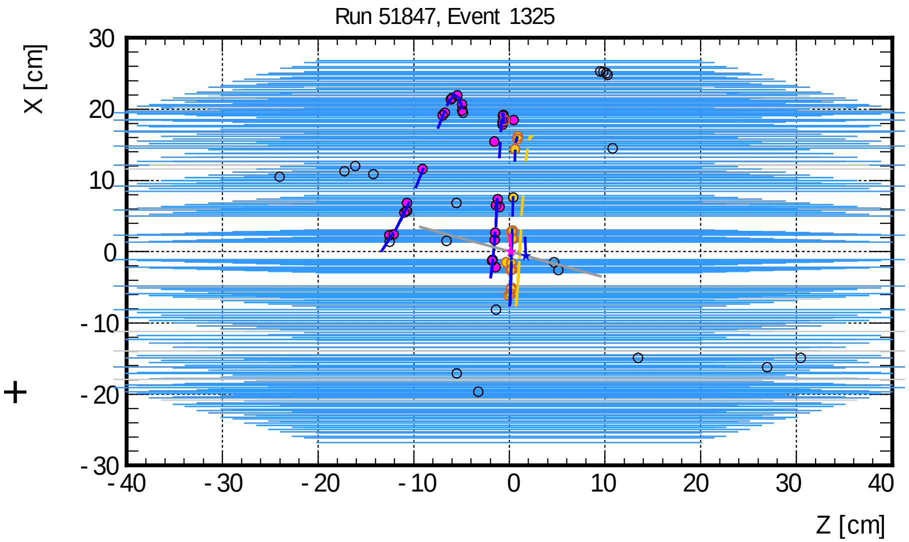

効果

- 2周目を認識できなかったため、イベント選別から漏れてしまったイベントの回復。 約4%のイベント増加
- AccBG イベントの出現と消滅はほぼ同数のため、BG数に対する影響は無い。

$\theta_{e\gamma}$, $\phi_{e\gamma}$, $t_{e\gamma}$

μ 粒子の初期位置($\boldsymbol{r}_\mu$)は飛跡がターゲットと交わる点とする。

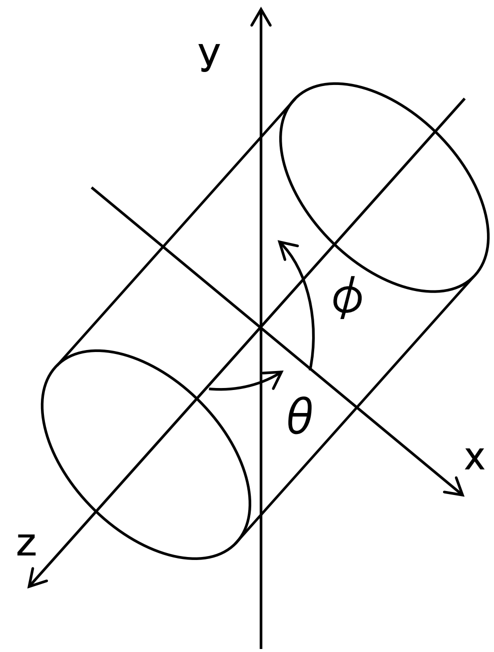

γ の放出角度　$$\boldsymbol{n}_\gamma = \frac{\boldsymbol{r}_\gamma - \boldsymbol{r}_\mu}{|\boldsymbol{r}_\gamma - \boldsymbol{r}_\mu|}$$

角度差 (0だと完全に反対向き)

$$\theta_{e\gamma} = (\pi - \theta_e) - \theta_\gamma$$
$$\phi_{e\gamma} = (\pi + \phi_e) - \phi_\gamma$$

時間差

$$t_{e\gamma} = \left(t_{\mathrm{LXe}} - \frac{|\boldsymbol{r}_\gamma - \boldsymbol{r}_\mu|}{c}\right) - t_e$$

PMT再構成

PMTごとのヒット再構成

constant fraction法から、ヒット時間

フィルターした波形を積分して、光子数を得る

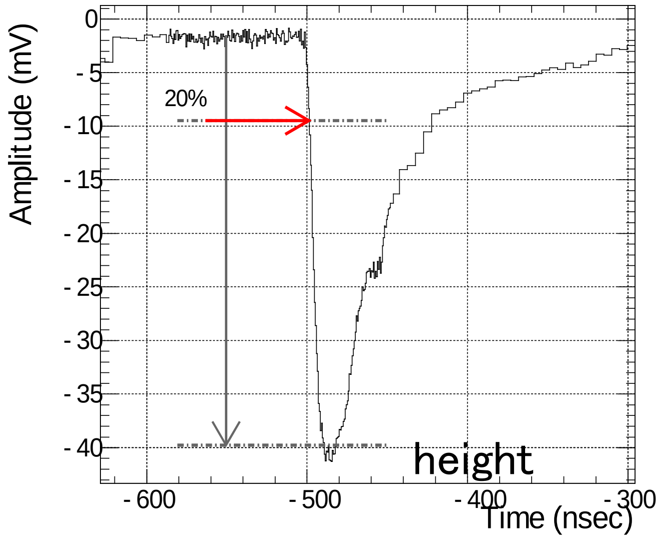

raw

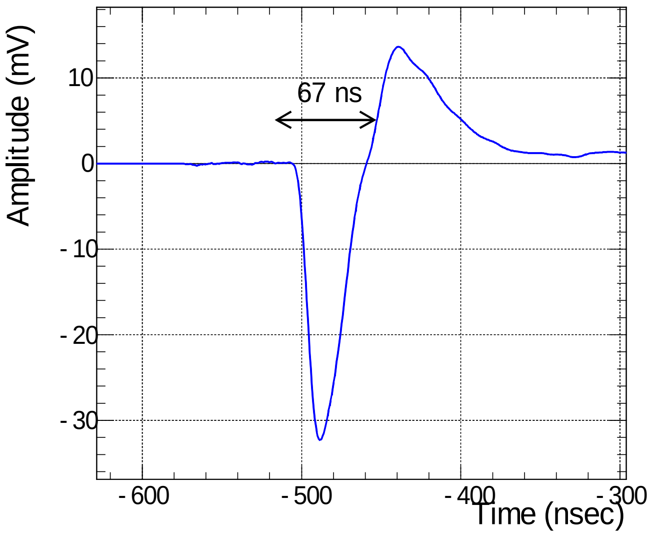

high-pass

LXe検出器 PMTの較正

増倍率(ゲイン)

LEDを一定の強度で点灯させる

$\sigma_N^2 = \mu_N + \sigma_0^2$ (N:光電子数)

$Q = G \times N$ で電荷の関係に直すと

$\sigma_Q^2 = G(\mu_Q + \sigma_0^2)$

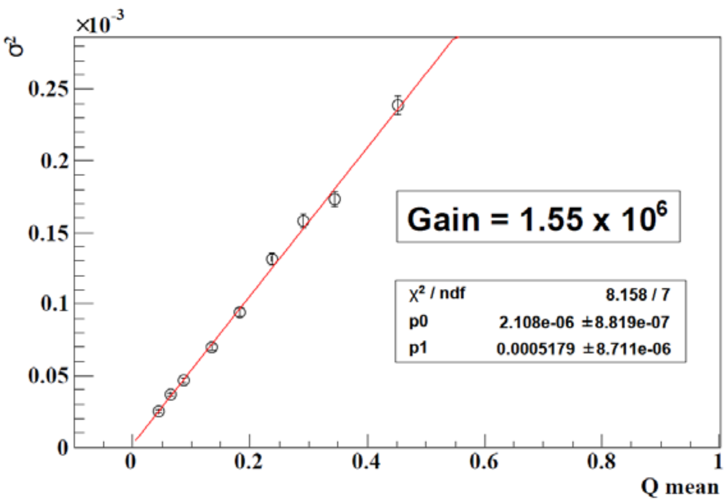

量子効率(QE)

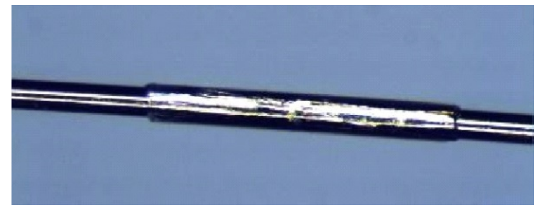

α線源(^{241}Am)が付いたワイヤー

α線イベントで測定された光電子数と、MCシミュレーションで予想される光子数の比からQEを計算する。

【新】γ線位置補正

2015年、
レーザー測量機を用いて検出器の内外壁、
PMT取付用の構造体を測量した。

結果、
x軸: 1 mrad, y軸: 5 mrad 程度の回転他、
図面からのズレが見つかった。

対策、
PMTの取付方法＋温度変化に基づいた位置の補正を行う。
(キセノンの重量による変形は無視できる)
修正されるガンマ線位置の平均値は、
角度の不確かさと同程度。(約4mrad)

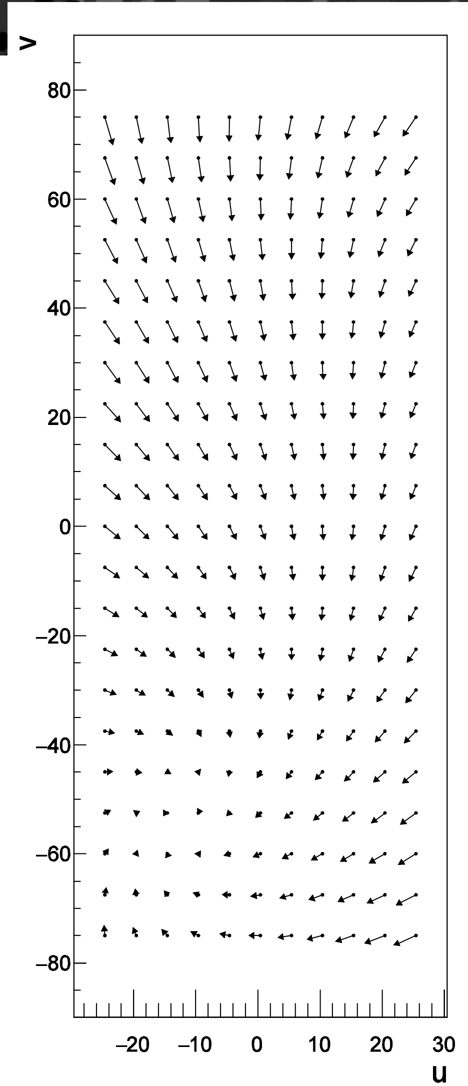

補正によるu,v位置
の移動(10倍)

ドリフトチェンバー位置合わせ

- Optical method
  - 測量器
    各年のrun開始前
    精度 0.2–0.3mm (x,y) 1.5–2.5mm (z)
  - レーザートラッカー とcorner cube
    2011年から
    精度 0.3mm (x,y,z)

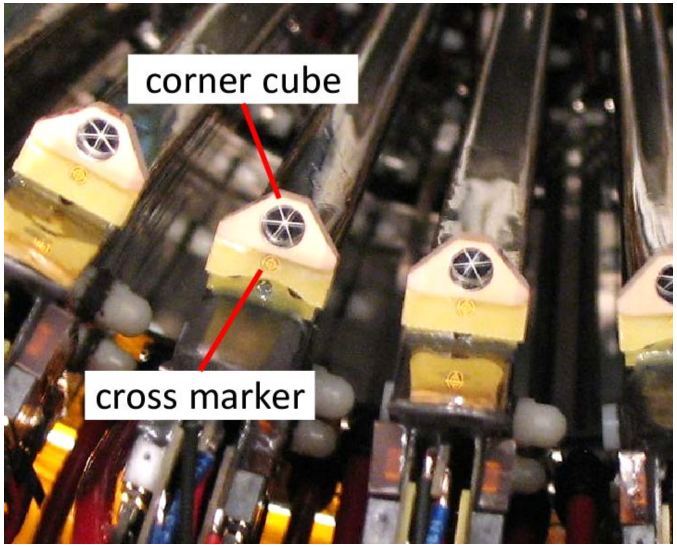

- Software method
  - Millipede alignment
    宇宙線カウンタ(CRC)を用いた特殊run
    精度 0.15mm
  - Michel positron alignment
    通常の陽電子trackとfitの残差が小さくなるよう
    最適化

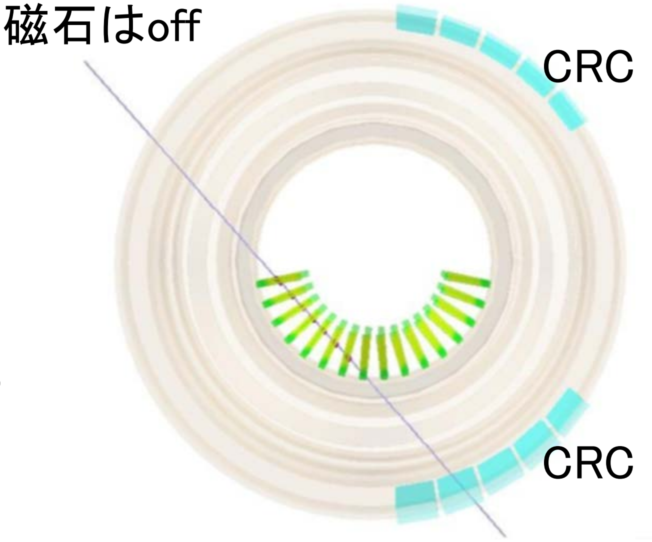

規格化因子の計算

Michel 法

通常崩壊陽電子の個数

$$k_{\text{Michel}} = \frac{N^{\text{Michel}}}{f_{Ee}^{\text{Michel}}} \times \frac{P_{\text{Michel}}}{\varepsilon_{\text{trg}}^{\text{Michel}}} \times \frac{\varepsilon_e^{\text{signal}}}{\varepsilon_e^{\text{Michel}}} \times A_\gamma^{\text{signal}} \times \varepsilon_{\text{trg}}^{\text{signal}} \times \varepsilon_{\text{sel}}^{\text{signal}}$$

trigger数

e⁺検出効率

γ 受入効率

trigger
効率

signal
選別効率

RMD 法

輻射崩壊の個数

$$k_{\text{RMD}} = \frac{N^{\text{RMD}}}{\mathcal{B}_{Ee}^{\text{RMD}}} \times \frac{\varepsilon_e^{\text{Signal}}}{\varepsilon_e^{\text{RMD}}} \times \frac{\varepsilon_{\text{trg}}^{\text{signal}}}{\varepsilon_{\text{trg}}^{\text{RMD}}} \times \frac{\varepsilon_{\text{sel}}^{\text{signal}}}{\varepsilon_{\text{sel}}^{\text{RMD}}}$$

e⁺検出効率

trigger
効率

signal
選別効率

どちらの方式も陽電子が検出されているイベント数からスタートするため、陽電子検出効率は既に含まれている。

平均PDFのフィットとの比較

角度変数を1次元化、event-by-eventでないPDFを用いる別解析と結果を比較した。フィット結果は、主方式と同様シグナルの有意な超過は無い。同じデータを別の方法で解析した上限値は多数のMCの分布の中心付近に位置する。

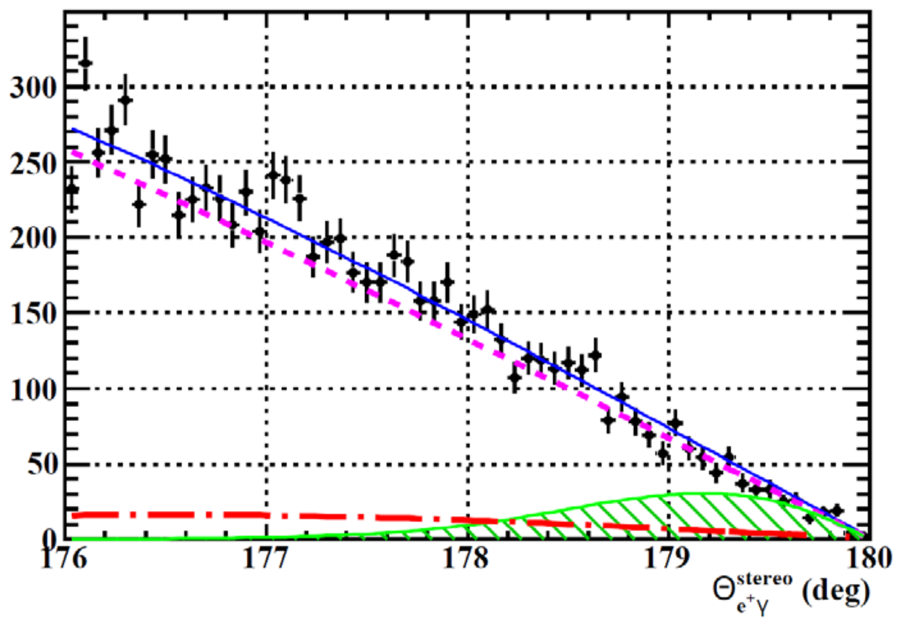

Θ (stereo angle) PDF とデータ

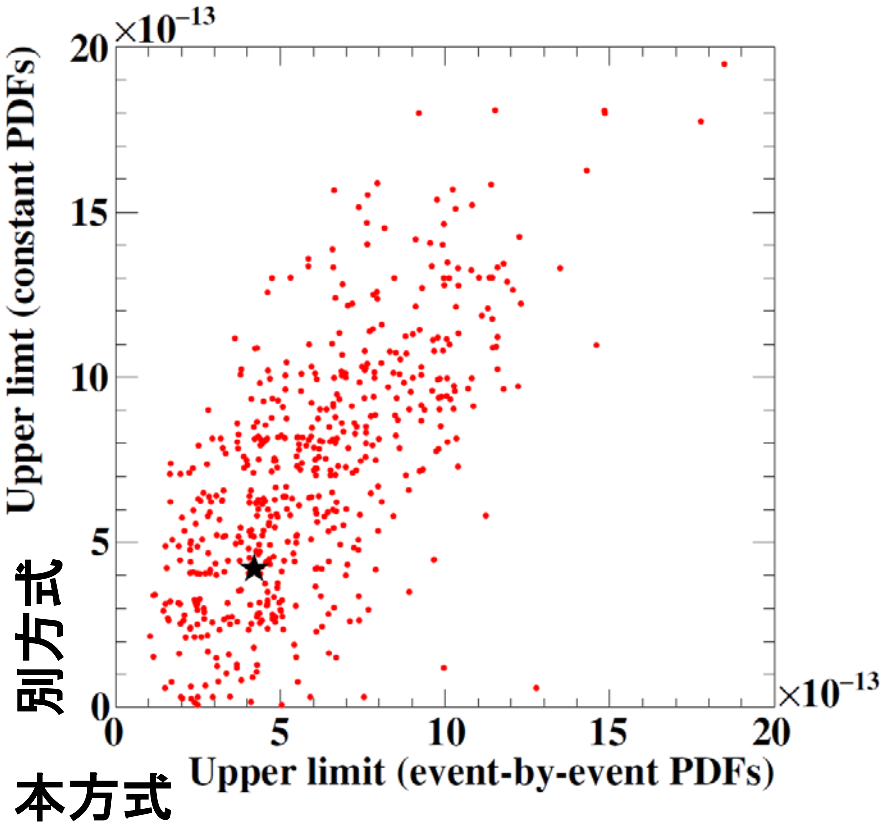

High rank events

Rank	Run	Event	Pair	Rsig	t [ps]	Ee [MeV]	Eg [MeV]	th [mrad]	ph [mrad]	cos	AIF
1	77431	1715	2	3.06	141.6	52.934	53.98	−25.19	−2.40	−0.99968	15
2	195187	1856	21	2.70	−75.0	53.338	51.74	−0.13	−9.19	−0.99996	7.4
3	189150	1089	25	2.41	−5.6	52.187	52.95	10.56	16.57	−0.99981	5.1
4	160737	785	10	2.31	47.6	52.816	51.92	8.30	6.12	−0.99995	8.3
5	56081	35	13	2.26	−22.2	52.524	52.81	−20.70	15.85	−0.99967	10
6	167931	1076	17	2.25	415.0	53.184	53.78	−7.67	−23.61	−0.99969	10
7	228740	1892	28	2.23	398.0	52.955	50.55	−0.83	−5.72	−0.99998	10
8	123579	1318	15	2.23	−20.7	52.806	55.13	−33.56	12.99	−0.99936	10
9	185612	1612	6	2.18	13.2	52.816	55.41	12.87	−29.79	−0.99948	10
10	87743	1484	24	2.15	−80.7	52.914	52.28	−18.08	23.97	−0.99955	4.3
11	218877	862	14	2.11	79.2	52.782	50.59	18.64	−9.77	−0.99978	10
12	113706	175	7	2.10	87.9	52.078	53.01	1.64	1.43	−1	10
13	185590	975	6	2.02	−57.1	53.009	52.59	−38.58	−3.11	−0.99925	3.5
14	194581	1185	17	2.01	−65.1	52.703	51.83	3.86	10.88	−0.99994	10
15	181128	1391	5	1.98	77.2	52.696	52.24	21.64	9.12	−0.99973	15
16	193209	1452	18	1.92	−310.1	52.708	54.83	−3.93	12.69	−0.99991	10
17	64033	592	5	1.83	157.5	53.385	49.65	19.15	6.12	−0.9998	10
18	100452	1878	6	1.81	−28.7	52.860	49.27	−14.59	21.97	−0.99965	13.3
19	111484	647	5	1.80	45.7	52.896	49.66	19.14	−23.65	−0.99954	15
20	84066	879	14	1.79	−61.9	52.759	51.31	−28.50	16.55	−0.99946	10